

**Hydrodynamic Behavior of Geldart particles type B and D in semi  
circular fluidized bed**

By

Muhammad Shukri Zulkefli

11169

Dissertation submitted in partial fulfillment of

the requirements for the

Bachelor of Engineering (Hons)

(Chemical Engineering)

MAY 2012

Universiti Teknologi PETRONAS

Bandar Seri Iskandar

31750 Tronoh

Perak Darul Ridzuan

## CERTIFICATION OF APPROVAL

**Hydrodynamic Behavior of Geldart particles type B and D in semi circular fluidized bed**

**By**

**Muhammad Shukri Zulkefli**

A project dissertation submitted to the  
Chemical Engineering Programme  
Universiti Teknologi PETRONAS  
in partial fulfillment of the requirement for the  
BACHELOR OF ENGINEERING (Hons)  
(CHEMICAL ENGINEERING)

Approved by,



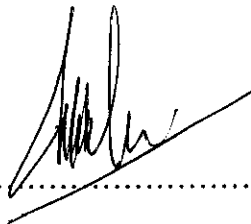
(Name of main supervisor)

**ASSOC. PROF. DR. MU ZILAFI MU SHABRI**  
Chemical Engineering Department  
Universiti Teknologi PETRONAS

**UNIVERSITI TEKNOLOGI PETRONAS**  
TRONOH, PERAK  
May 2012

## CERTIFICATION OF ORIGINALITY

This is to certify that I am responsible for the work submitted in this project, that the original work is my own except as specified in the references and acknowledgements, and that the original work contained herein have not been undertaken or done by unspecified sources or persons.



.....  
MUHD SHUKRI ZULKEFLI

890831-10-5813

K 1169

CHEMICAL ENGINEERING

## **ABSTRACT**

Geldart particles type B and D range from 100  $\mu\text{m}$  and more. Green bean, urea and rice will be experiment material because it has size over than 100  $\mu\text{m}$ . Due to that, experimental work will focus on hydrodynamic behavior of Geldart particles where bubble diameter, bed expansion and minimum fluidizing air velocity will be study. Semi-circular fluidized bed will be the experiment equipment. Result from the experiment will be compared in graph with different colour line that indicate different dimaeter of material.

To capture hydrodynamic behavior of bubble, high speed camera, SONY XC 75CE CCD will be used and put in front of the fluidized bed. Image analysis software was used to analyse the image captured via the high speed camera. Pictures taken with the high speed camera will be set to 200 pps, exposure 4997.25 and resolution 1280 x 720.

## **ACKNOWLEDGEMENT**

First and foremost, thank you to Allah S.W.T for the time and guidance that He gave to me to complete this final year project that consume one year to complete. Allah the most merciful and compassionate. All praise to the Almighty.

I would like to express my deep gratitude to my supervisor Dr Ku Zilati Ku Shaari who kindly assists me throughout the project. Her supervision, endless support, guidance and help to me during the undertaken the project is highly appreciated.

I would also like to thank the staff of Mechanical Engineering, Mr. Khairul Anwar Bin Haji Ahmad for the kind co operation and supervision to allow me to use lab in block 15 and his supervision while using high speed camera.

Last but not least, I would like to thank all my friends who helped me to complete this project.

# Table of Contents

CHAPTER 1 .....	5
INTRODUCTION .....	5
1.1 BACKGROUND STUDY .....	5
Figure 1.1: Classification of Geldart particles .....	5
1.2 PROBLEM STATEMENT.....	8
1.3 OBJECTIVES AND SCOPE OF STUDY .....	9
CHAPTER 2 .....	10
LITERATURE REVIEW .....	10
2.1 FLUIDIZED BED .....	10
2.2 MINIMUM AIR-FLUIDIZATION VELOCITY .....	11
Figure 2.2.1: Effect of pressure versus minimum fluidization velocity (Rowe et al 1984)..	14
2.3 BED EXPANSION.....	16
Figure 2.3.1: Bed expansion versus minimum fluidization at different pressure (a) Group B solids (b) Group D solids ( Schweinzer and Molerus 1987).....	17
2.4 EFFECT OF DIFFERENT PARTICLES .....	18
CHAPTER 3 .....	19
METHODOLOGY .....	19
3.1 PROCEDURE .....	19
3.1.1 Apparatus setup .....	19
Figure 3.1 : Fluidized bed circular and semi-circular .....	19
Figure 3.2 : Experiment set up used in the video imaging through the rectangular column ( Ganeshkumar Subramaniam,2003).....	20
Figure 3.3: Experiment set up with high speed camera,SONY XC 75CE CCD with setting 200 frames per second, exposure 4997.5 and resolution 1280 X 720 .....	20
3.1.2 Experimental Procedure.....	21
3.1.3 Experimental Matrix.....	23
Table 3.1: Detailed condition of each experimental run. The results are then compared and analyzed.....	23

CHAPTER 4 .....	24
RESULTS AND DISCUSSION.....	24
4.1 Minimum fluidization velocity, $U_{mf}$ .....	24
Table 4.1: Density of air at room temperature but different pressure.....	24
Table 4.2: Minimum fluidization of $D_p$ 0.34mm,2.71mm,3.35mm at different pressure. ...	25
Figure 4.1: Min fluidization, $U_{mf}$ versus pressure for $D_p$ 0.34mm,2.71mm,3.35mm .....	25
4.2 Effect of pressure to the bed expansion .....	26
Table 4.3: Bed expansion for $D_p = 0.34$ mm.....	26
Table 4.4 : Bed expansion for $D_p = 2.71$ mm.....	26
Table 4.5: Bed expansion for $D_p = 3.35$ mm.....	26
Figure 4.2 : Expanded bed height versus pressure (bar) for particles diameter 0.34mm,2.71mm and 3.35mm, $H_{mf} = 10$ cm .....	27
4.2 Effect of different particles to the bubble diameter .....	28
Table 4.6: Bubble diameter for $D_p = 0.34$ mm.....	28
Table 4.7: Bubble diameter for $D_p = 2.71$ mm.....	28
Table 4.8: Bubble diameter for $D_p = 3.35$ mm.....	29
Figure 4.3 : Bubble diameter(cm) versus height for $D_p$ 0.35mm,2.71mm,3.35mm at pressure 0.3 bar , $H_{mf} = 10$ cm,20cm,30cm .....	29
Figure 4.4 : Bubble diameter(cm) versus height for $D_p$ 0.34mm, 2.71mm,3.35mm at..... pressure 0.5 bar, $H_{mf} = 10$ cm, 20cm,30cm .....	30
Figure 4.5 : Bubble diameter(cm) versus height for $D_p$ 0.34mm, 2.71mm, 3.35mm at pressure 0.7 bar, $H_{mf} = 10$ cm,20cm,30cm .....	30
Figure 4.6: Bubble diameter(cm) versus height for $D_p$ 0.34mm,2.71mm,3.35mm at pressure 0.9bar, $H_{mf} = 10$ cm,20cm,30cm .....	31
Figure 4.7: Bubble diameter(cm) versus pressure for $D_p$ 0.34mm,2.71mm,3.35mm at $H_{mf} = 10$ cm .....	32
Figure 4.8: Bubble diameter(cm) versus pressure for $D_p$ 0.34mm,2.71mm,3.35mm at $H_{mf} = 20$ cm .....	32
Figure 4.9: Bubble diameter(cm) versus pressure for $D_p$ 0.34mm,2.71mm,3.35mm for $H_{mf} = 30$ cm. ....	33
CHAPTER 5 .....	34
CONCLUSION AND RECOMMENDATION.....	34
5.1 Conclusion.....	34
5.2 Recommendation .....	35

REFERENCES .....	36
APPENDIX .....	40
Figure 1: Bubble diameter distribution for height above air distributor, $D_p = 2.71\text{mm}$ , Pressure = 0.3 bar, $H_{mf} = 10\text{cm}$ .....	40
Figure 5 : Bubble diameter distribution for height above air distributor, $D_p = 2.71\text{mm}$ Pressure = 0.5 bar, $H_{mf} = 20\text{cm}$ .....	42
Figure 7 : Bubble diameter distribution for height above air distributor $D_p = 2.71\text{mm}$ Pressure = 0.7 bar, $H_{mf} = 10\text{cm}$ .....	43
Figure 8 : Bubble diameter distribution for height above air distributor $D_p = 2.71\text{mm}$ Pressure = 0.7 bar, $H_{mf} = 20\text{cm}$ .....	44
Figure 9 : Bubble diameter distribution for height above air distributor $D_p = 2.71\text{mm}$ Pressure = 0.7 bar, $H_{mf} = 30\text{cm}$ .....	44
Figure 10 : Bubble diameter distribution for height above air distributor $D_p = 2.71\text{mm}$ Pressure = 0.9 bar, $H_{mf} = 10\text{cm}$ .....	45
Figure 11 : Bubble diameter distribution for height above air distributor $D_p = 2.71\text{mm}$ Pressure = 0.9 bar, $H_{mf} = 20\text{cm}$ .....	46
Figure 12 : Bubble diameter distribution for height above air distributor $D_p = 2.71\text{mm}$ Pressure = 0.9 bar, $H_{mf} = 30\text{cm}$ .....	46
Figure 13 : Bubble diameter distribution for height above air distributor $D_p = 3.35\text{mm}$ Pressure = 0.3 bar, $H_{mf} = 10\text{cm}$ .....	47
Figure 14 : Bubble diameter distribution for height above air distributor $D_p = 3.35\text{mm}$ Pressure = 0.3 bar, $H_{mf} = 20\text{cm}$ .....	47
Figure 15 : Bubble diameter distribution for height above air distributor $D_p = 3.35\text{mm}$ Pressure = 0.3 bar, $H_{mf} = 30\text{cm}$ .....	48
Figure 16 : Bubble diameter distribution for height above air distributor $D_p = 3.35\text{mm}$ Pressure = 0.5 bar, $H_{mf} = 10\text{cm}$ .....	48
Figure 17 : Bubble diameter distribution for height above air distributor $D_p = 3.35\text{mm}$ Pressure = 0.5 bar, $H_{mf} = 20\text{cm}$ .....	49
Figure 18 : Bubble diameter distribution for height above air distributor $D_p = 3.35\text{mm}$ Pressure = 0.5 bar, $H_{mf} = 30\text{cm}$ .....	49
Figure 19 : Bubble diameter distribution for height above air distributor $D_p = 3.35\text{mm}$ Pressure = 0.7 bar, $H_{mf} = 10\text{cm}$ .....	50
Figure 20 : Bubble diameter distribution for height above air distributor $D_p = 3.35\text{mm}$ Pressure = 0.7 bar, $H_{mf} = 20\text{cm}$ .....	50
Figure 21 : Bubble diameter distribution for height above air distributor $D_p = 3.35\text{mm}$ Pressure = 0.7 bar, $H_{mf} = 30\text{cm}$ .....	51

Figure 22: Bubble diameter distribution for height above air distributor $D_p = 3.35\text{mm}$ Pressure = 0.9 bar, $H_{mf} = 10\text{cm}$ .....	51
Figure 23 : Bubble diameter distribution for height above air distributor $D_p = 3.35\text{mm}$ Pressure = 0.9 bar, $H_{mf} = 20\text{cm}$ .....	52
Figure 24 : Bubble diameter distribution for height above air distributor $D_p = 3.35\text{mm}$ Pressure = 0.9 bar, $H_{mf} = 30\text{cm}$ .....	52
Figure 25: Project Gant Chart.....	2

# CHAPTER 1

## INTRODUCTION

### 1.1 BACKGROUND STUDY

Geldart's particle was introduced by Professor D. Geldart that proposed powders were grouping according to the "Geldart Groups". The groups are defined based on diagram of solid-fluid density difference and particle size.

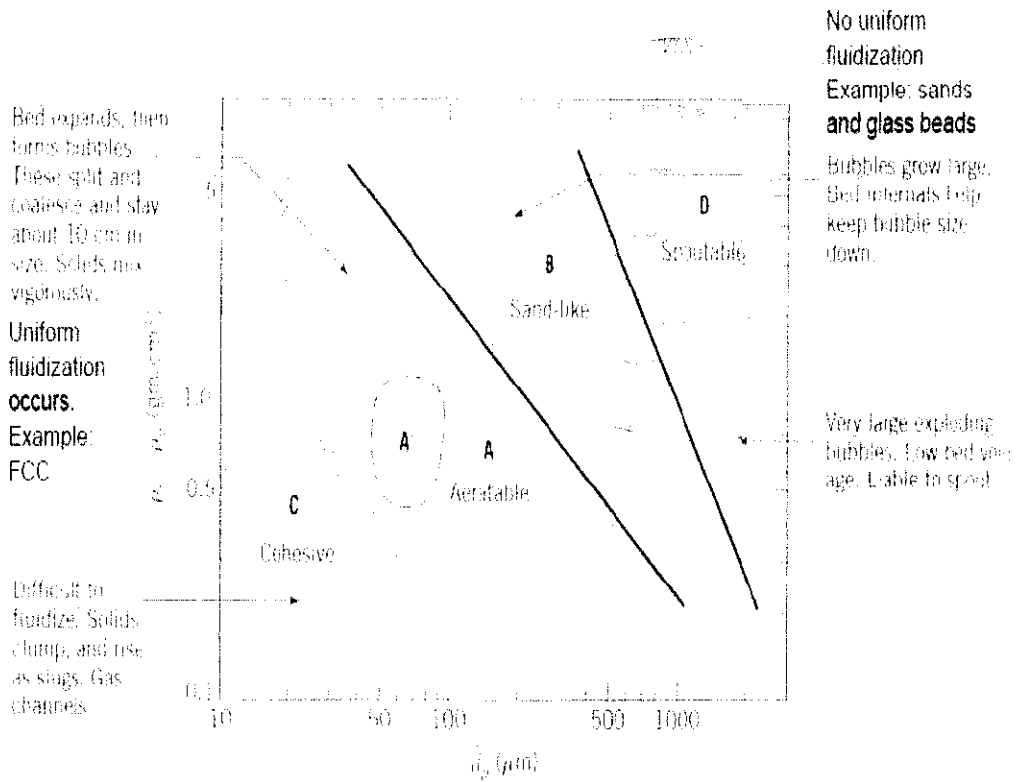


Figure 1.1: Classification of Geldart particles

From the picture above it is clearly shown there are four types of Geldart's group namely Geldart's C particle, Geldart's A particle, Geldart's B particle and Geldart's D particle which arranged according to their respective particle sizes.

Group C particles is cohesive. It's difficult to fluidized and channeling can occurs. Interparticle forces greatly affect the fluidization behavior of these powders. Mechanical powder compaction prior to fluidization greatly affected the fluidization behavior of the powder, even after the powder had been fully fluidized for a while. Saturating the fluidization air with humidity reduced the formation of agglomerates and greatly improved the fluidization quality. The water molecules adsorbed on the particle surface presumably reduced the van der Waals forces. Range of particle's diameter is from 0-30 $\mu\text{m}$ . Flour and cement are examples for this group.

Group A is aeratable and been characterized by a small  $d_p$  and small  $p_p$ . Large bed expansion occur before bubbling starts. Gross circulation of powder even if only a few bubbles are present. In the emulsion phase, large gas backmixing can happen. Rate at which gas is exchanged between the bubbles and the emulsion is high. Bubble size can be reduced by either using a wider particle size distribution or reducing the average particle diameter. The particle's diameter range for this group is between 30-100  $\mu\text{m}$ . Example for group A is milk flour .

Group B is bubbling and solids recirculation rates are smaller. Less gas back mixing in the emulsion phase. Rate at which gas is exchanged between bubbles and emulsion is smaller. Bubble size is almost independent of the mean particle diameter and the width of the particle size distribution. For this group there is no observable maximum bubble size. Particle's diameter range is around 100-1000  $\mu\text{m}$  and sand can be example for group B.

Group D is spoutable. Bubbles coalesce rapidly and flow to large size. Bubbles rise more slowly than the rest of the gas percolating through the emulsion. The dense phase has a low voidage. Range of particle diameter for this particular group is over than 1000  $\mu\text{m}$ . For group D coffee bean and wheat are the examples.

For this research, only particles that fall into Group B and D ( coarse particles) will be study in the circular and semi-circular fluidized bed. The particles that will be taken into consideration to be use during the experiment are urea, rice and green bean. Urea, a white crystalline solid is one of the most important component in agricultural industry. With current technology, urea is manufactured as granules. It is added to the soil to release nutrients necessary for plant to growth. Use of conventional fertilizers may lead to concentration levels that are too high for effective action. According to Kiran J.K et al [1] mention that high concentration may produce undesirable side effects in the target area, which could lead to crop damage, or in the surrounding environment . To increase effectiveness of fertilizers and avoid environmental risk, Slow-release fertilizers (SFR) is used. According to Tzika.M et al [2] mention that Slow-release fertilizers (SFR) have been recently been developed aiming at retarding the release rate of the nutrients to the ground. For rice and green bean, it is very familiar to the cooking world where many dishes can be create using this two ingredients.

## 1.2 PROBLEM STATEMENT

Fluidized beds are very significant to the industrial world which include pharmaceutical industry, chemical and petrochemical industry, combustion or pyrolysis, for advance material such as silicon production and nano carbon tubes. There are plenty types of fluidized bed in the industry that being classified by their flow behavior. Among examples of fluidized bed are Wurster fluidized bed, Swirling fluidized bed and pressurized fluidized bed but for this research semi-circular fluidized reactor will be use.

This research was carried out to study the hydrodynamic behavior of Geldart particles group B and D in the semi-circular fluidized bed reactor. During fluidization, bubble formation inside the reactor will be observed. It is important to examine bubble formation in the fluidized bed to increase the efficiency of contact between gas and solids.

According Sobrino. C et al [6] due mention that it is important task to control the bubble size to avoid large and fast bubbles that by-pass the bed and increase the elutriation. Bubble characteristics such as bubble size, shape or ascending velocity are important parameters that had been extensively study in the past.

This project is very significant because result from this study can be use by industry to improve the efficiency of fluidized bed in their plant especially semi circular fluidized bed. Despite that, bubbles behavior in semi-circular type of fluidized bed that involve Geldart particles group B and D can be known. In a nutshell, via this study can identify hydrodynamic behavior of Geldart particles group B and D

### **1.3 OBJECTIVES AND SCOPE OF STUDY**

The research will study about the hydrodynamic behavior of the Geldart's particle group B and D where objectives of the project are stated below:

1. To obtain minimum fluidizing air velocity in semi circular fluidized bed
2. To determine effect of pressure to the bed expansion of semi circular fluidized bed
3. To study effect of different particles (Geldart's B and D) to the bubble diameter in the semi circular fluidized bed.

## **CHAPTER 2**

### **LITERATURE REVIEW**

#### **2.1 FLUIDIZED BED**

Fluidized bed is commonly use in chemical industry for a various process such as coating, drying, granulation, combustion oxidation and chlorination. Flow behaviors in the fluidized bed solely depend on result of fluid-particle and particle-particle interaction. Hilal. N (2004) said that characteristic of fluidized bed depend upon the behavior of gas bubbles that generated near the distributor and rise through the growing in size and becoming fewer by coalescence.

According to Li.H et al (2003) mention that the fluidization can be divided into two classes which are aggregative fluidization and particulate fluidization. Aggregative fluidization appears in gas-solids system where the particle distribution in the gas is not uniform. Gas bubbles and solids agglomerate did exist. Heat and mass transfer rate are low due to contact between gas and solids is not good.

Meanwhile particulate fluidization appears in liquid-solids systems where this type of fluidization has more uniform particles distribution in the liquid and bubbles and agglomerates do not form. Liquid and solids contact are very good and thus result in high heat and mass transfer rate. According to Singh R.K et al (2005) mention that particulate fluidization exists between minimum fluidization velocity and minimum bubbling velocity. Minimum bubbling velocity is the superficial gas velocity at which first bubble first appear.

Sobrinho C. et al(2007) had conducted an experiment which involve fluidization of Group B particles with a rotating distributor. Fluidization sometimes difficult to achieve due to the agglomeration or cohesion between particles. Despite that, defluidization or non-uniform fluidization may occur sometimes.

Despite the agglomeration problems, some researchers due suggest few solutions. Sobrinho.C et al( 2007) suggested vibrated bed where better mixing between gas and particles can be achieved. Li.H et al(2003) mention two groups of method (1) particle and fluid design and (2) external force field, internals and configuration design. This two method can increase the reaction efficiency of gas-solids fluidization.

## 2.2 MINIMUM AIR-FLUIDIZATION VELOCITY

Minimum fluidization velocity  $U_{mf}$  is the velocity at which fluidization start to begin. According to Lim K.S et al(1995), minimum fluidization velocity is based on the balance of pressure drops required to support the weight minus buoyancy acting on the particles at the point of minimum fluidization. Based on the Ergun's equation, minimum fluidization velocity  $U_{mf}$  is calculated using the equation below:

$$Re_{mf} = \sqrt{C_1^2 + C_2 Ar} - C_1$$

$$Re_{mf} = (\rho_G d_p U_{mf}) / \mu_G$$

$$Ar = (\rho_G \Delta p g d_p^3) / \mu_G^2$$

Where  $\Delta p = (\rho_p - \rho_G)$  is the pressure drop,  $\rho_p$  is the particle density,  $\rho_G$  is the gas density,  $d_p$  is the particle diameter ,  $\mu_G$  is the gas viscosity,  $U_{mf}$  is the minimum fluidization velocity,  $Re_{mf}$  is the Reynolds number  $Ar$  is the Archimedes number and  $C_1, C_2$  is the particle shape dependant and species dependant.

Besides the equation mentioned earlier, minimum fluidization velocity  $U_{mf}$ , also can be found using Ergun's equation directly by substituting superficial fluid velocity with  $U_{mf}$  and the pressure drop across the bed is equal to the effective weight per unit area of the particles at the point of incipient fluidization as per below:

$$\frac{\Delta P}{L} = 150 \frac{(1 - \varepsilon_{mf})^2}{\varepsilon_{mf}^3} \frac{\mu U_{mf}}{(\phi_s d_p)^2} + 1.75 \frac{(1 - \varepsilon_{mf}) \rho_g U_{mf}^2}{\varepsilon_{mf}^3 \phi_s d_p}$$

Where  $\Delta P$  is equal to the bed weight per unit cross-sectional area, and the particle sphericity,  $\phi_s$  is defined as the surface area of a volume equivalent sphere divided by the particle's surface area. When applying the Ergun equation, one has to know the minimum fluidization voidage,  $\varepsilon_{mf}$  although it is frequently an unknown.

Other than Ergun's equation, one of the more widely used correlations to predict  $U_{mf}$  is the Wen and Yu Correlation (1966). The simplified form of the Wen and Yu correlation is :

$$Ar = 1650 Re_{p,mf} + 24.5 (Re_{p,mf})^2$$

Above equation can be rearranged to form equation below. This form expresses  $U_{mf}$  in terms of known system parameters.

$$U_{mf} = \frac{\mu}{\rho_g d_p} \left[ \frac{(33.7)^{0.5} + 0.0408 d_p^3 \rho_g (\rho_p - \rho_g) g}{\mu^2} \right]^{0.5}$$

Where  $Ar$  is Archimedes number,  $Re$  is Reynold's number,  $\mu$  is air viscosity,  $\rho_g$  is gas density,  $d_p$  is particle diameter,  $g$  is gravity 9.81 m/s and  $\rho_p$  is particle density.

The effect of temperature and pressure on  $U_{mf}$  is strongly influenced by particle size. For small particles ( $Re_{p,mf} < 20$ ), the simplified Wen and Yu Equation reduces to:

$$U_{mf} = \frac{d_p^2(\rho_p - \rho_g)g}{1650\mu}$$

For large particles ( $Re_{p,mf} > 1000$ ),

$$U_{mf} = \frac{d_p(\rho_p - \rho_g)g}{24.5\rho_g}$$

Rang R. Pattipati and C.Y. Wen (1981) said that the minimum fluidization velocity decreases with increasing temperature for small particles. They also mention that for small particles and at high temperature, the viscous forces are dominant. However, for larger particles, kinetic forces are dominant compared to viscous force.

According to Vojtěch V. et al (1966), a fixed bed is a layer of particles which rest on one another and do not move relative to one another or relative to the walls of the container. On the other hand, moving bed is a layer of particles moving as a whole under the action of gravity. After reach fluidization state, the volume of the bed is somewhat larger than the volume of the fixed layer. Thus, the bed is said to be expand. If we further increases the velocity of the fluid, the bed continues to expand, the height of the bed increases. However, the concentration of particles per unit volume of the bed decrease.

Once the minimum fluidization velocity can be obtain, the next stage can be proceed where velocity will be increase gradually and the effects to bubble formation will be record. Air fluidization velocity very important parameter. Moderate air fluidization velocities can give uniform bubble formation since the particles will follow regular flow trajectories while their respective collision rate was negligible.

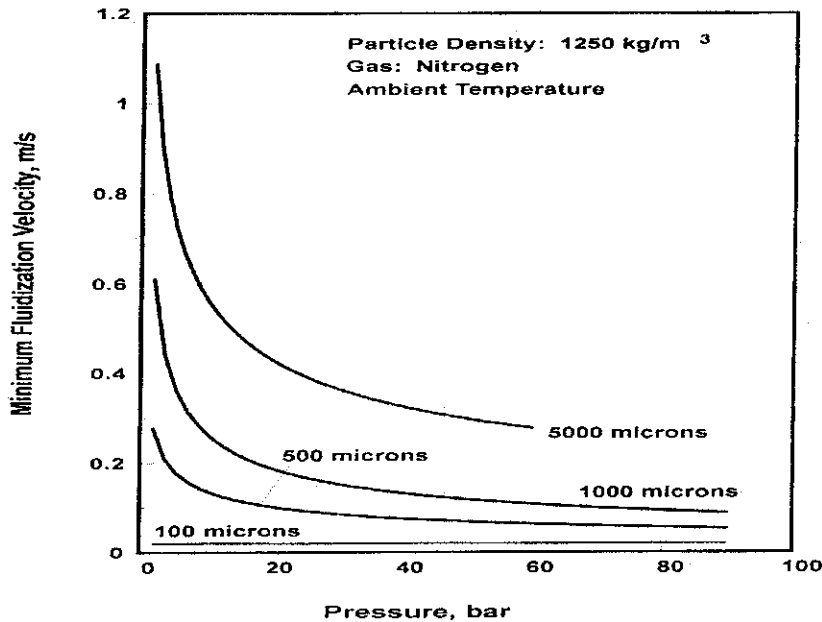


Figure 2.2.1: Effect of pressure versus minimum fluidization velocity (Rowe et al 1984)

Based on Figure 2.2.1, experiment conducted by Rowe et al (1984) had shown that the minimum fluidization velocity will decrease when pressure increase. The heavier particles 5000 microns, 1000 microns and 500 shown very much decrease in minimum fluidization velocity when pressure increase while the lighter particles 100 microns do not shown very much decrease. Increment in pressure do not affect significantly the minimum fluidization velocity for lighter particles.

Tzika. M et al (2003) has conducted experiments with the effect of the air-fluidization velocity. The air fluidization velocity was varied by moving the position of the flap at the air outlet. At position 0 (completely open flap) the velocity of the air was the

lowest. As the flap was gradually shut 35 %, 45% and 60%, it gave different results. When air fluidization velocity was very low ( flap position of 35%) the granules did not follow a uniform flow trajectory, while frequency granules entered coating zone significantly reduced. This resulted in the formation of a quite thin, nonuniform coating. For air-fluidization at high velocity (flap position of 60%), the granules entered coating zone more often and granule's mean residence time in the coating zone per pass was reduced. Hence it result in poor coating quality.

According to Sidorenko. I et al (2004) mention that in industrial practice fluidized bed reactors are mostly operated at superficial gas velocities well above the minimum fluidization velocities. Therefore, the minimum fluidization velocity is not very applicable in the industry.

## 2.3 BED EXPANSION

Bed expansion in semi-circular fluidized bed depends largely on the size of the fluidized bed. Particles distribution in the gas is not uniform hence exist gas bubbles and solid particles agglomerates. This affect the heat and mass transfer rate where it becomes low. Several researchers have proposed several correlations to predict bed expansion such as two-phase theory, growth of the bubbles and via correlation of experimental data.

In the study of L.lop M.F et al (1999), bed expansion has influence on the residence time in a chemical reactor, bubble growth, mass transfer phenomena and can determine the height of any heat exchange equipment.

Few experiments had been conducted by researchers about bed expansion in the fluidized bed. Experiment conducted by Kawabata et al (1981) shows that the expansion increased with pressure for Geldart B from the observation of bubble diameter and velocity in bed.

Experiment conducted by Hilal. N (2004) study the effect of particle bed depth. The dimensionless bed density for 325  $\mu\text{m}$  Diakon particles is given for bed depths of 200,300,400 and 500 mm in the 290 mm diameter bed. From the experiment, Hilal. N (2004) notice that the difference of particles depth at difference level is smalls and not systematic.

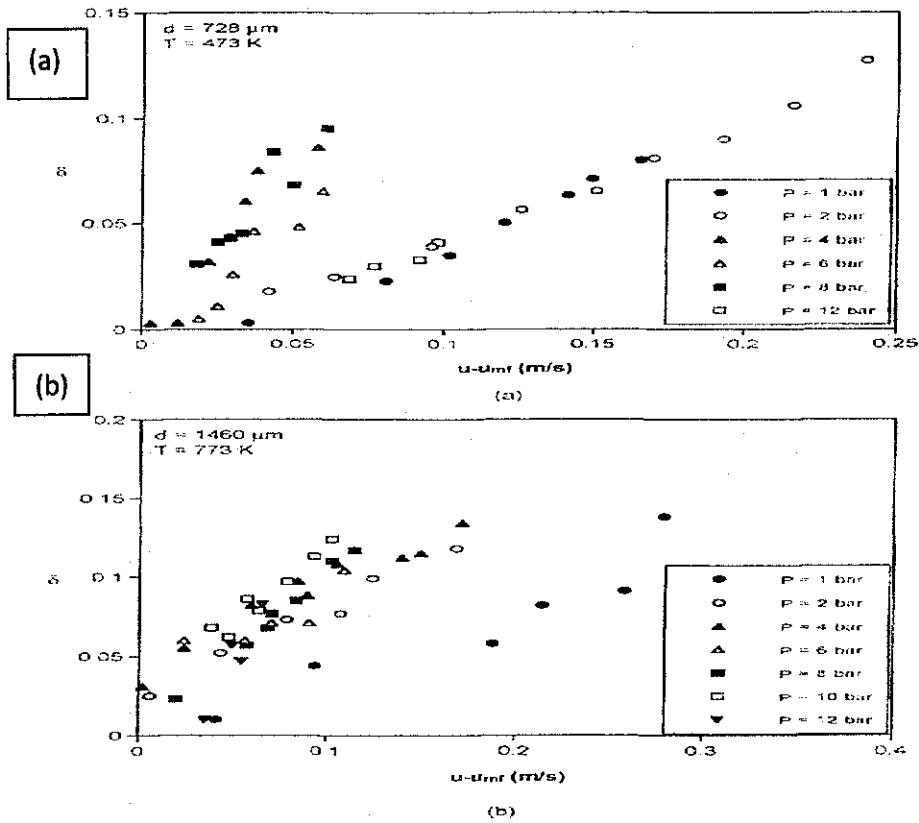


Fig. 1 Bed expansion versus  $u-umf$  at different pressures. (a) Group B solids, (b) Group D solids.

Figure 2.3.1: Bed expansion versus minimum fluidization at different pressure (a) Group B solids (b) Group D solids ( Schweinzer and Molerus 1987)

Figure 2.3.1 above shown the bed expansion at different pressure for group B and group D solids. Schweinzer and Molerus(1987) observed that bubble fraction therefore bed expansion was not significantly influenced by pressure for Group B particles, nevertheless by analyzing the visible flow of bubbles as well as bubble diameter and velocity, it can be concluded that bed expansion increased with pressure for particles belonging to groups B and D.

## **2.4 EFFECT OF DIFFERENT PARTICLES**

In the experiment, different particles will be used namely rice with  $D_p$  0.34mm, green bean with  $D_p$  2.71mm and urea with  $D_p$  3.35mm. Experiment will be conducted in semi-fluidized bed.

Sidorenko. I. et al (2004) mention that particles size do bring effect to the minimum fluidization velocity and pressure. The result from the experiment did show a decrease in the minimum fluidization velocity with increasing pressure for particles larger than 100  $\mu\text{m}$  (Geldart particles type B and D).

Hilal.N (2004) found only certain type of particles types can be effectively fluidized. Isometric particles smaller than 10  $\mu\text{m}$  display cohesive properties that usually prevent uniform fluidization while particles in the range of 10 -100  $\mu\text{m}$  of low density fluidized in a particulate manner of the minimum velocity of fluidization.

According to Tao Zhou et al (1999) mention that fluidized bed characteristic really get affected by the size of the particles which the smaller particles size, bigger inter-particle force therefore the worse fluidized behavior.

## CHAPTER 3

### METHODOLOGY

#### 3.1 PROCEDURE

The overall methodology of this study are divided into three parts which are

- i. Apparatus setup
- ii. Experimental procedure
- iii. Experimental matrix

##### 3.1.1 Apparatus setup

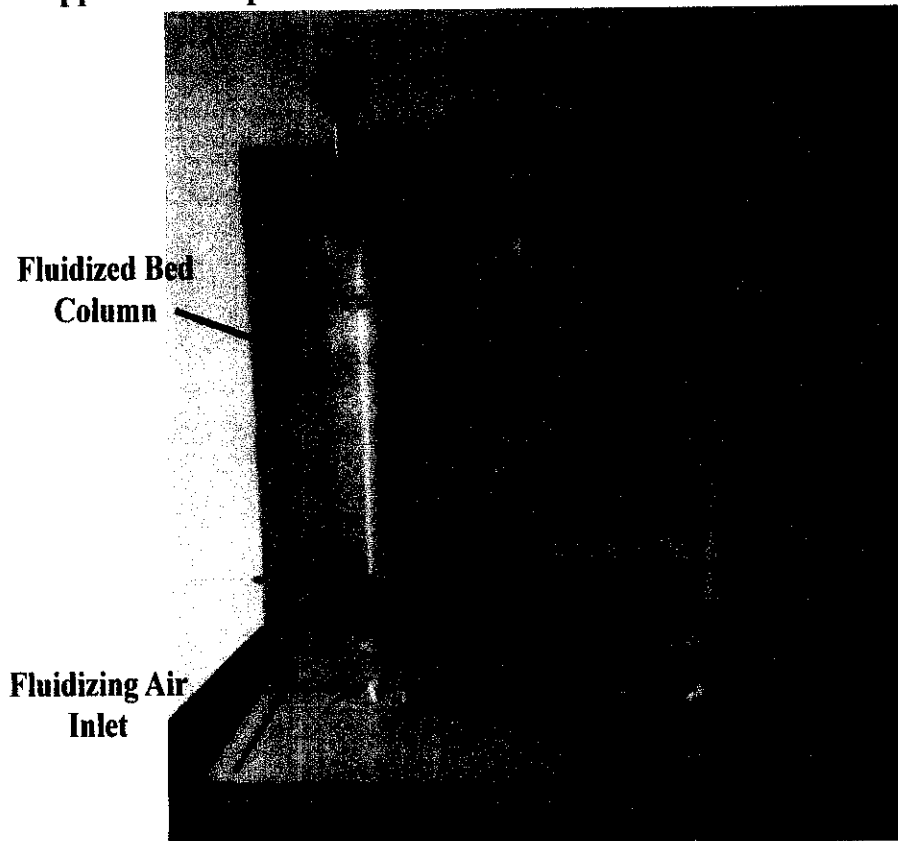


Figure 3.1 : Fluidized bed circular and semi-circular

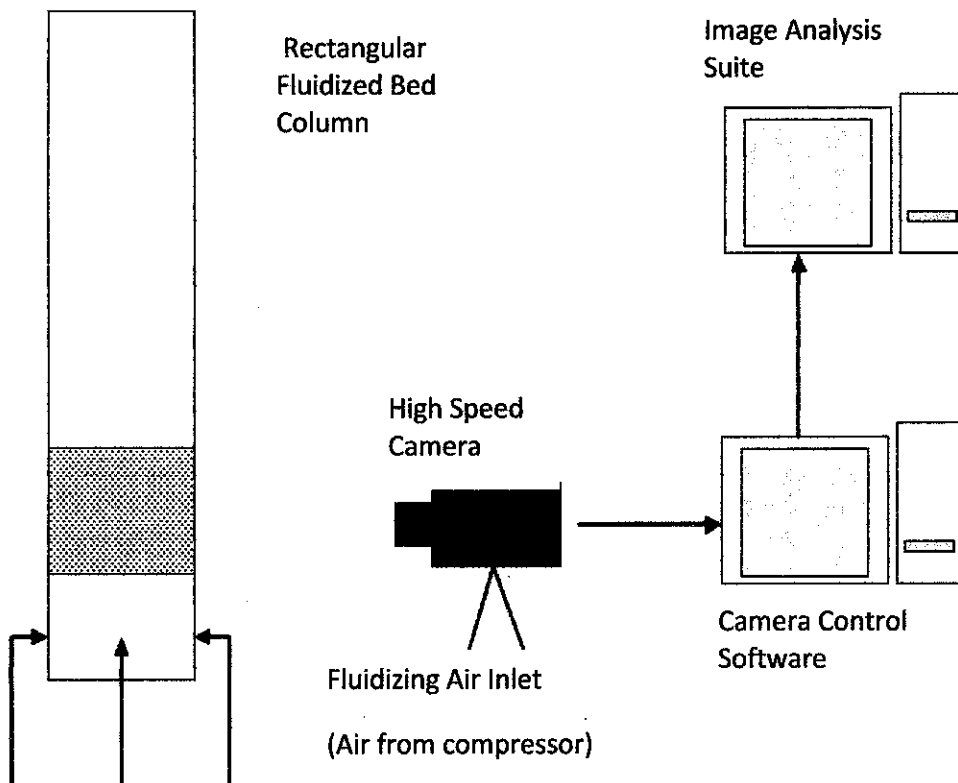


Figure 3.2 : Experiment set up used in the video imaging through the rectangular column ( Ganeshkumar Subramaniam,2003)

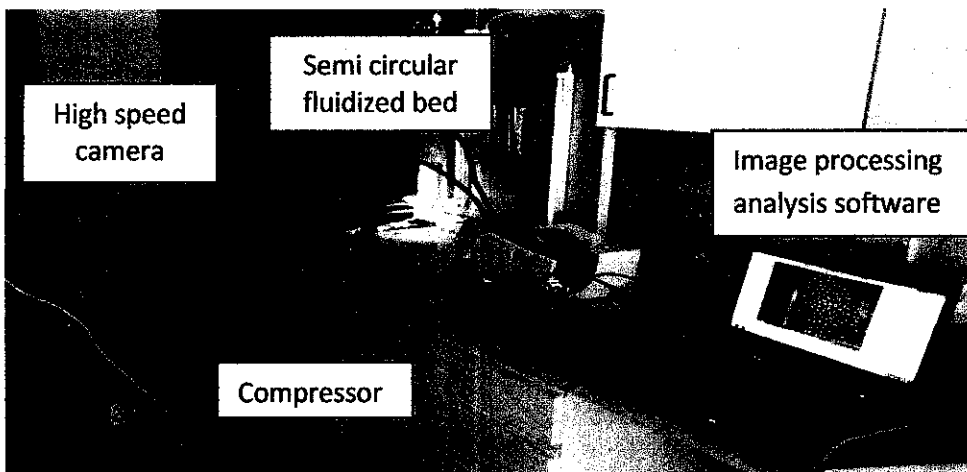


Figure 3.3: Experiment set up with high speed camera,SONY XC 75CE CCD with setting 200 frames per second, exposure 4997.5 and resolution 1280 X 720

### 3.1.2 Experimental Procedure

The experiment consist of a semi-circular column with 50 cm height and 5.7cm in diameter, a syringe and air compressor to provide the fluidizing medium (gas) to establish required superficial gas velocity, and camera Sony XC 75CE CCD, Sony Inc.

The distributor plates are made from wire mesh tray with pore size of 20  $\mu\text{m}$  and a fractional free area of 60%. Granular urea, green bean and rice are used as the Geldart's particles. The particles are divided into Geldart's particles specification such as, Geldart B, and Geldart D. The bubble formation of the particles in the fluidized bed is investigated by changing the pressure and particles sizes.

The experiment set up is according to figure 3.2 and figure 3.3. Fill the semi circular fluidized bed with one type of Geldart particle. Measure the bed height and the value is the initial bed height. Air from compressor was feed to the rectangular shape plenum which located beneath the distributor plate. Let the air flow for five minutes and the take the inlet pressure and outlet pressure. The process was recorded by using high speed camera at 200 frames per second. High speed camera was placed in front of the fluidized bed to capture the dynamic images. Save the images captured and analyze. The fluidizing air from the compressor flows into the fluidized bed through the bottom plate and fluidized the particles by overcoming the centrifugal force. Fluidized bed must be in line with the camera lens in order to capture the fluidization images.

The air flow rates will be increase to get increment in pressure. The bed height was adjusted by removing or adding Geldart particles to or from the bed to get the desired bed height. The experiment was repeated with different Geldart particles. To study effect of pressure to bed expansion, the bed height was fixed with 10cm with

increment in pressure 0.5 bar, 0.7 bar, 0.9 bar and 1.1 bar. To study effect of different particles to bubble diameter, the bed height was 10cm, 20cm and 30cm for each pressure different.

Voidage measurements were obtained in a given region of interest of the bed using a single CCD camera mounted perpendicular to the flat front face of the bed. A shutter of 0.1 ms was used in order to obtain crisp, blur-free images. The software counted the number of tablets in the FOV automatically. To convert the number count to a voidage, the depth of field, DOF, of the camera and lens system had to be found.

The DOF was obtained by calibration and using this value with the known volume of tablets in a given volume of bed, the local void volume in the bed was calculated. (Subramaniam, 2003). All steps are repeated using different atomizing air pressure, different Geldart's particles group, different fluidized column and different type of distributor. The results are compared and analyzed.

### 3.1.3 Experimental Matrix

Experiments	Type of Fluidized Bed Column	Type of Particle	Fluidizing Air Pressure (bar)	Initial Bed Height (cm)
Effect of pressure to bed expansion				
Run 1	Semi-Circular	Geldart's B & D	0.5	10
Run 2			0.7	10
Run 3			0.9	10
Run 4			1.1	10
Effect of different particles to bubble diameter				
Run 5	Semi-Circular	Geldart's B & D	0.5	10
Run 6			0.5	20
Run 7			0.5	30
Run 8			0.7	10
Run 9			0.7	20
Run 10			0.7	30
Run 11			0.9	10
Run 12			0.9	20
Run 13			0.9	30
Run 14			1.1	10
Run 15			1.1	20
Run 16			1.1	30

Table 3.1: Detailed condition of each experimental run. The results are then compared and analyzed.

## CHAPTER 4

### RESULTS AND DISCUSSION

#### 4.1 Minimum fluidization velocity, $U_{mf}$

Minimum fluidization velocity can be find via calculation and few information need to be fill in the equation. At 1 bar and room temperature, 22C.\*Density of air =1.199 kg/m<sup>3</sup>.\*Viscosity of air = 1.825 X 10<sup>-5</sup>.Volume semi circular = 127.58 cm<sup>3</sup>.Diameter semi circular fluidized bed = 5.7cm, Length semi circular fluidized bed = 50cm

	<b>Urea</b>	<b>Green Bean</b>	<b>Rice</b>
<b>Particle diameter, Dp</b>	3.35mm	2.71mm	0.34mm
<b>Weight(kg)</b>	0.4	0.35	0.22
<b>Density (kg/cm<sup>3</sup>)</b>	3135	2743	1724

Table 4.1: Density of air at room temperature but different pressure

<b>Pressure (bar)</b>	<b>Air density (kg/m<sup>3</sup>)</b>
0.5	1.9414
0.7	2.178
0.9	2.452
1.1	2.712

\* value of air density and viscosity is based on

[http://www.engineeringtoolbox.com/air-temperature-pressure-density-d\\_771.html](http://www.engineeringtoolbox.com/air-temperature-pressure-density-d_771.html)

By using Wen and Yu equation,  $U_{mf}$  can be calculated.

$$U_{mf} = \frac{\mu}{\rho_g d_p} \left[ \frac{(33.7)^{0.5} + 0.0408 d_p^3 \rho_g (\rho_p - \rho_g) g}{\mu^2} \right]^{0.5}$$

Simplified version Wen and Yu equation

For small particles ( $Re < 20$ )

$$U_{mf} = \frac{d_p^2(\rho_p - \rho_g)g}{1650\mu}$$

For large particles ( $Re > 1000$ )

$$U_{mf} = \frac{d_p(\rho_p - \rho_g)g}{24.5\rho_g}$$

Table 4.2: Minimum fluidization of  $D_p$  0.34mm, 2.71mm, 3.35mm at different pressure.

Pressure(bar)	$U_{mf}$ for $D_p$ 3.35mm (m/s)	$U_{mf}$ for $D_p$ 2.71mm (m/s)	$U_{mf}$ for $D_p$ 0.34mm (m/s)
0.5	1.47	1.24	0.35
0.7	1.38	1.16	0.33
0.9	1.38	1.10	0.31
1.1	1.24	1.05	0.29

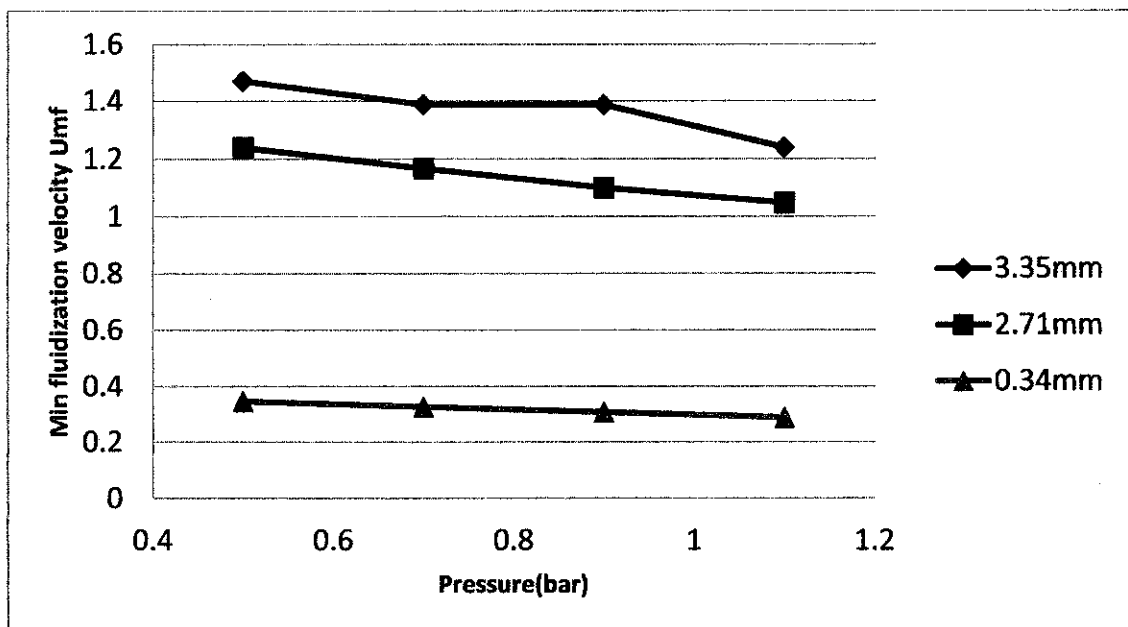


Figure 4.1: Min fluidization,  $U_{mf}$  versus pressure for  $D_p$  0.34mm, 2.71mm, 3.35mm

Effect of pressure and temperature on minimum fluidization velocity,  $U_{mf}$  largely depend upon particle size. From Figure 4.1, it can be seen that increasing system pressure causes  $U_{mf}$  to decrease for particle size greater than 100  $\mu\text{m}$ . Materials of this size are essentially Geldart Group B and D. For large particles, the Wen and Yu equation predicts that  $U_{mf}$  should vary as  $(\frac{1}{\rho_g})^{0.5}$ . Therefore,  $U_{mf}$  should decrease with pressure for large particles.

#### 4.2 Effect of pressure to the bed expansion

The results are shown in table below. Bed height before the experiment is fix which is 10 cm.

Table 4.3: Bed expansion for  $D_p = 0.34$  mm.

Pressure (bar)			Expanded bed height (cm)
Inlet	Outlet	$\Delta P$	
0.5	0.11	0.39	19
0.7	0.10	0.6	21
0.9	0.12	0.78	27
1.1	0.21	0.89	34

Table 4.4 : Bed expansion for  $D_p = 2.71$  mm

Pressure (bar)			Expanded bed height (cm)
Inlet	Outlet	$\Delta P$	
0.5	0.09	0.41	17
0.7	0.1	0.6	20
0.9	0.11	0.79	25
1.1	0.15	0.95	32

Table 4.5: Bed expansion for  $D_p = 3.35$  mm

Pressure (bar)			Expanded bed height (mm)
Inlet	Outlet	$\Delta P$	
0.5	0.1	0.4	13
0.7	0.11	0.59	22
0.9	0.12	0.78	24
1.1	0.16	0.94	26

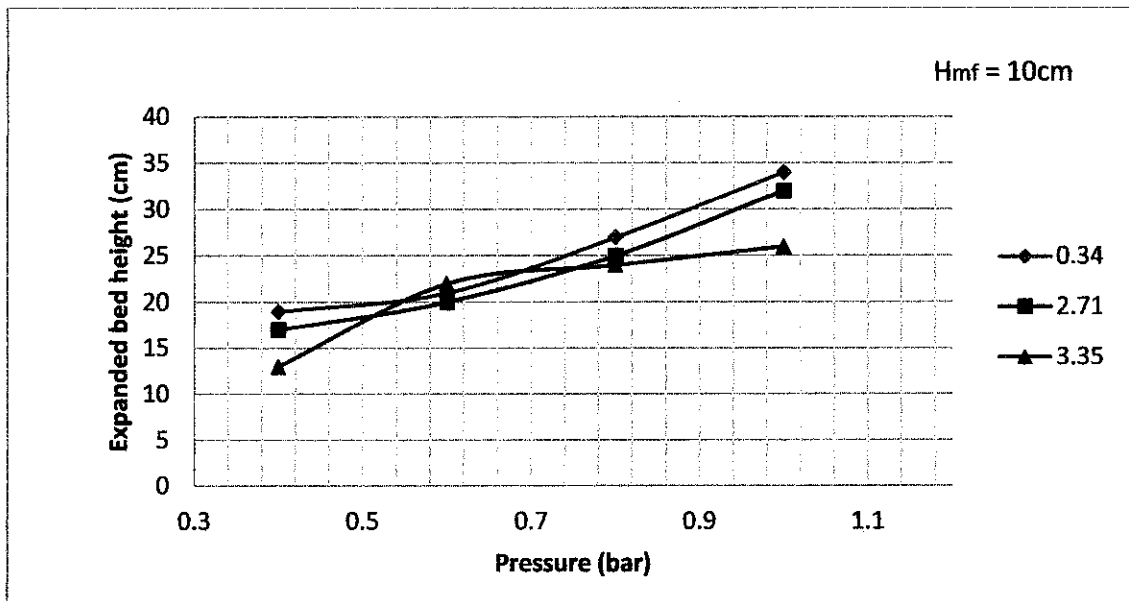


Figure 4.2 : Expanded bed height versus pressure (bar) for particles diameter 0.34mm,2.71mm and 3.35mm, **Hmf =10cm**

Based from the Figure 4.2, the result clearly shown that the bed expansion is increase with the increasing of pressure but bed expansion will decrease if heavier particles is used. Bed expansion for particles size 3.35mm and 2.71mm are shorter than 0.34mm. The bed new height decreased with the particle size.

## 4.2 Effect of different particles to the bubble diameter

Table 4.6: Bubble diameter for  $D_p = 0.34$  mm

Inlet	Pressure		Initial Bed Height (cm)	Bubble diameter(cm)
	Outlet	$\Delta P$		
0.5	0.12	0.38	10	3.2
	0.125	0.375	20	2.7
	0.12	0.38	30	4.4
0.7	0.16	0.54	10	2.9
	0.18	0.52	20	3.5
	0.17	0.53	30	4.0
0.9	0.18	0.72	10	2.6
	0.2	0.7	20	4
	0.19	0.71	30	6.0
1.1	0.2	0.9	10	1.5
	0.22	0.88	20	3.2
	0.21	0.89	30	6.2

Table 4.7: Bubble diameter for  $D_p = 2.71$  mm

Inlet	Pressure		Initial Bed Height (cm)	Bubble diameter(cm)
	Outlet	$\Delta P$		
0.5	0.12	0.38	10	2.9
	0.125	0.375	20	3.0
			30	4.1
0.7	0.16	0.54	10	2.7
	0.18	0.52	20	3.2
			30	3.9
0.9	0.18	0.72	10	3.1
	0.2	0.7	20	3.5
			30	5.2
1.1	0.2	0.9	10	2.4
	0.22	0.88	20	2.5
			30	5.4

Table 4.8: Bubble diameter for  $D_p = 3.35\text{mm}$

Inlet	Pressure		Initial Bed Height (cm)	Bubble diameter(cm)
	Outlet	$\Delta P$		
0.5	0.12	0.38	10	2.5
	0.125	0.375	20	2.7
	0.18	0.32	30	3.9
0.7	0.16	0.54	10	2.5
	0.18	0.52	20	2.9
	0.16	0.54	30	4.2
0.9	0.18	0.72	10	2.6
	0.2	0.7	20	3.2
	0.18	0.72	30	6.5
1.1	0.2	0.9	10	2.7
	0.22	0.88	20	1.5
	0.19	0.91	30	5.2

The graph of bubble diameter at certain height above air distributor for  $D_p$  0.34mm,2.71mm,3.35mm with pressure 0.3,0.5,0.7 and 0.9 bar are shown in Fig. 4.3, Fig 4.4, Fig 4.5 and Fig 4.6 below

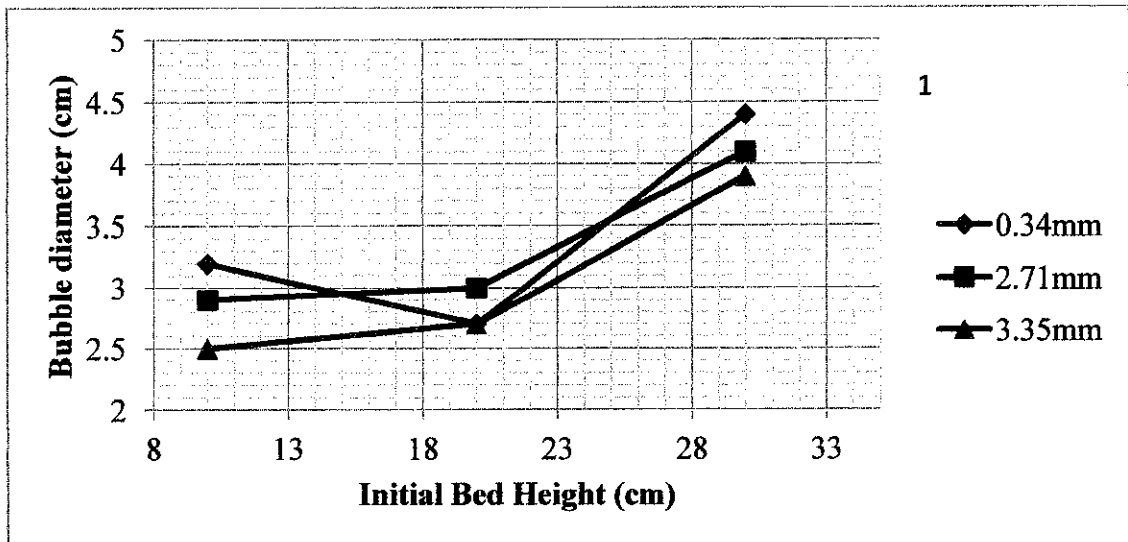


Figure 4.3 : Bubble diameter(cm) versus height for  $D_p$  0.35mm,2.71mm,3.35mm at pressure 0.3 bar ,  $H_{mf} = 10\text{cm}, 20\text{cm}, 30\text{cm}$

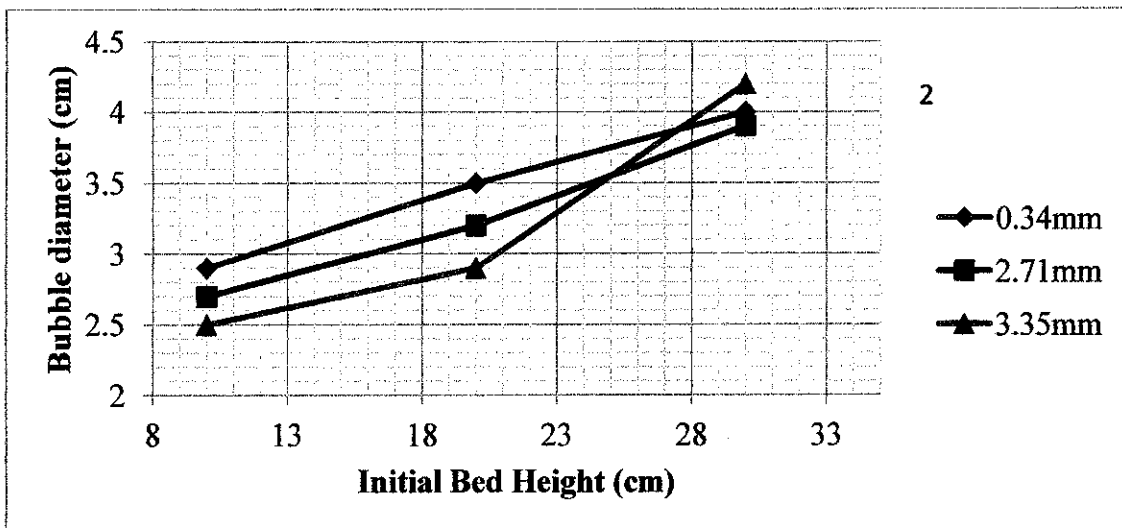


Figure 4.4 : Bubble diameter(cm) versus height for  $D_p$  0.34mm, 2.71mm, 3.35mm at pressure 0.5 bar,  $H_{mf} = 10\text{cm}, 20\text{cm}, 30\text{cm}$

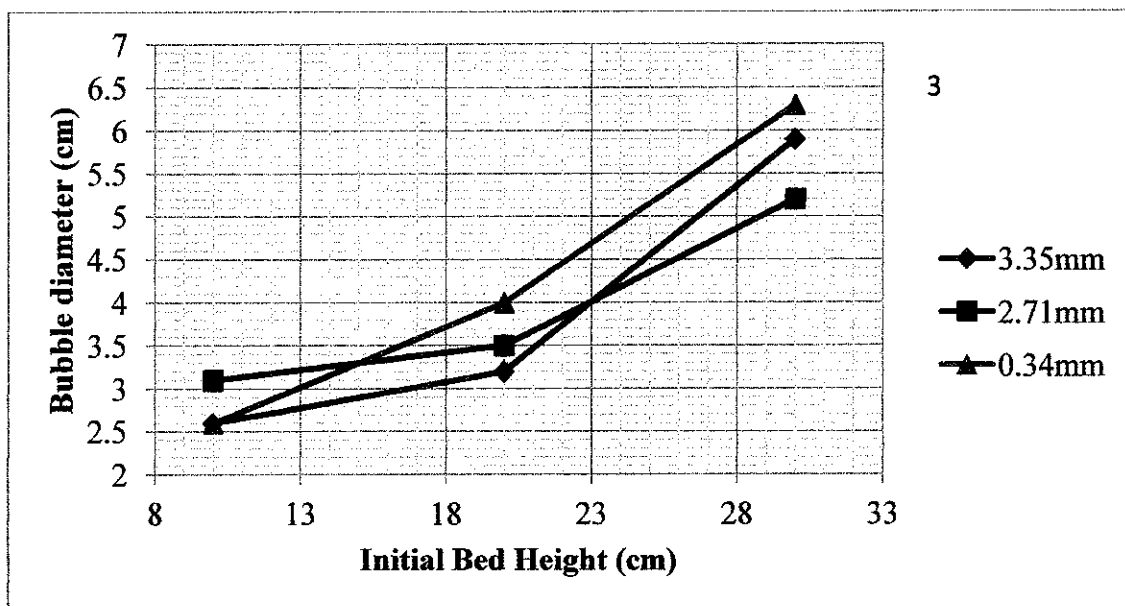


Figure 4.5 : Bubble diameter(cm) versus height for  $D_p$  0.34mm, 2.71mm, 3.35mm at pressure 0.7 bar,  $H_{mf} = 10\text{cm}, 20\text{cm}, 30\text{cm}$

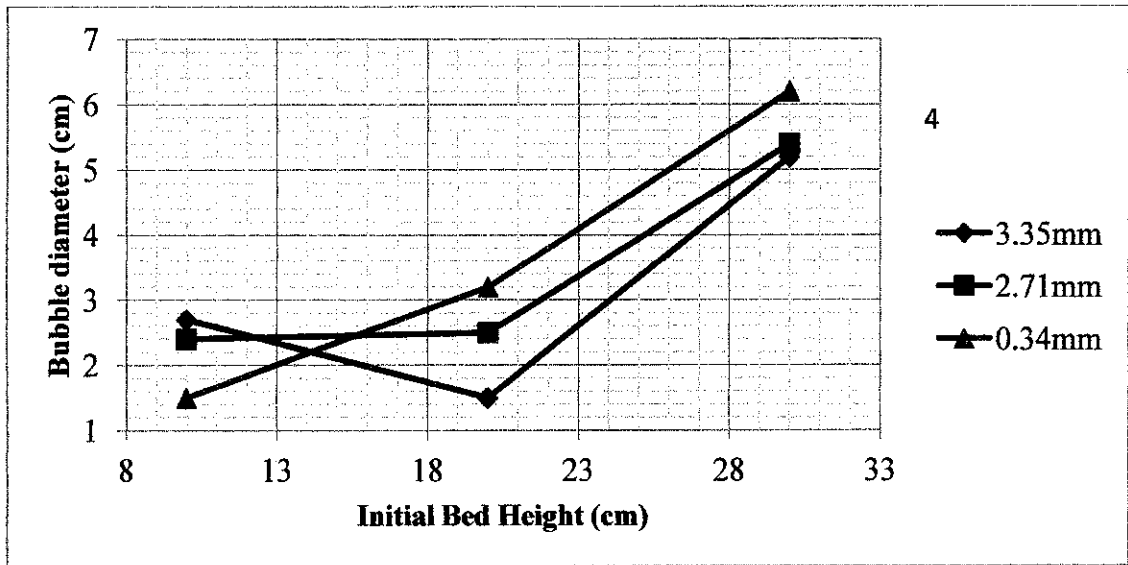


Figure 4.6: Bubble diameter(cm) versus height for Dp 0.34mm,2.71mm,3.35mm at pressure **0.9bar**,  $H_{mf}$ =10cm,20cm,30cm

The graph shown above indicate relation between different particles and its effect to the bubble diameter at different pressure namely 0.3 bar, 0.5 bar, 0.7 bar and 0.9 bar. Based on Fig. 4.3, Fig 4.4, Fig.4.5 and Fig 4.6, it can be concluded that particle size with Dp 0.34 mm show bubble size that is bigger than 2.71mm and 3.35mm. Smaller particles will form larger bubbles diameter.

As the height above air distributor increase, as can be seen from above graph, particles with Dp 0.34mm still predominates the graph that form large bubbles and then followed by Dp 2.71mm and Dp 3.35mm. Large particles will have larger void friction in packed bed column and thus affect the bubble diameter where the bubble diameter is happening to be smaller.

The graph of bubble diameter versus pressure can be seen below in Fig 4.7, Fig 4.8 and Fig 4.9 for  $D_p$  0.34mm, 2.71mm and 3.35mm with initial bed height 10cm, 20cm and 30cm.

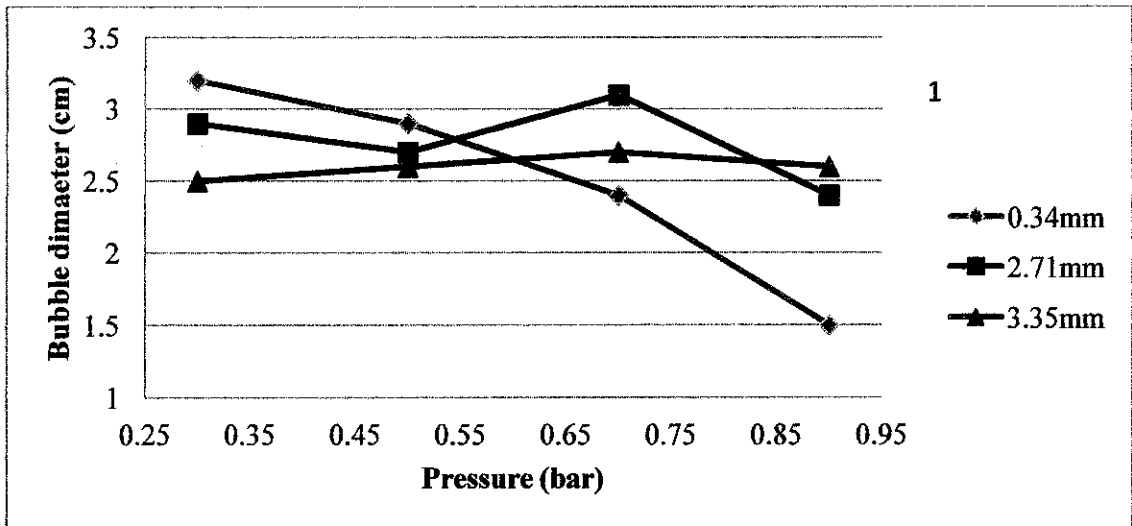


Figure 4.7: Bubble diameter(cm) versus pressure for  $D_p$  0.34mm, 2.71mm, 3.35mm at  $H_{mf}=10\text{cm}$

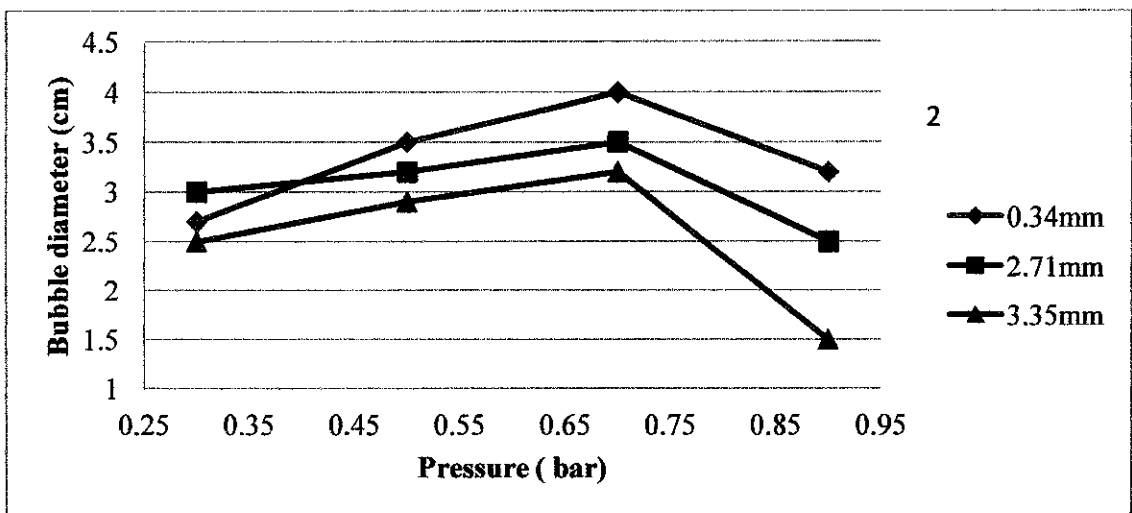


Figure 4.8: Bubble diameter(cm) versus pressure for  $D_p$  0.34mm, 2.71mm, 3.35mm at  $H_{mf}=20\text{cm}$

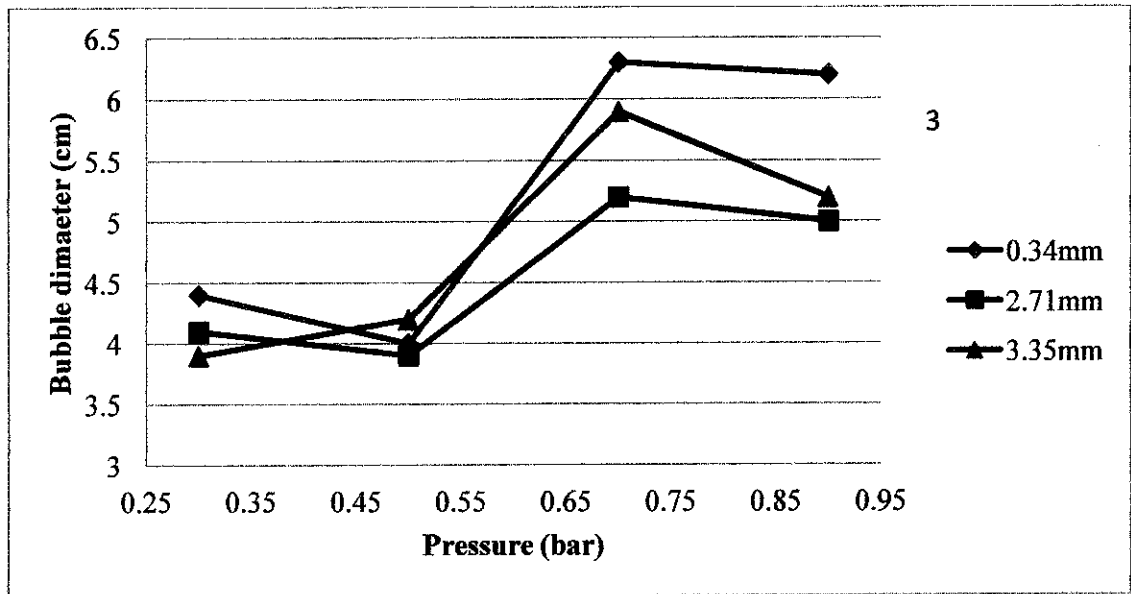


Figure 4.9: Bubble diameter(cm) versus pressure for  $D_p$  0.34mm, 2.71mm, 3.35mm for  $H_{mf}=30\text{cm}$ .

Based on Fig 4.7, Fig 4.8 and Fig 4.9, as the pressure increase the bubble diameter will increase gradually until certain pressure where bubble diameter is maximum and after that bubble diameter will decrease even though pressure is increasing. From the graph can be seen that bubble diameter is increasing when pressure increase from 0.3 bar to 0.5 bar to 0.7 bar. After 0.7 bar, bubble diameter decrease even though pressure increase at 0.9 bar. Particles with  $D_p$  0.34mm still predominates the graph that create large bubble. This is because smaller particles have smaller void friction that enable air to form larger bubbles.

## CHAPTER 5

### CONCLUSION AND RECOMMENDATION

#### 5.1 Conclusion

High speed camera was used in the experiment because it can capture fast moving particles via high shutter speed feature. Characteristic bubble formation in the fluidized bed can be studied via pictures taken via high speed camera.

Minimum fluidization velocity  $U_{mf}$  depends on particle size. For large particles, the Wen and Yu equation predicts that  $U_{mf}$  should vary as  $(\frac{1}{\rho_g})^{0.5}$ . Therefore,  $U_{mf}$  should decrease with pressure for large particles. Results from the experiment also show that as pressure increases, minimum fluidization velocity will decrease.

For expanded bed height, the results show that pressure did not have a significant effect on the bed height. As particle diameter increases, the expanded bed height will increase as well. Bed expansion for particle sizes 3.35mm and 2.71mm are shorter than 0.34mm. The bed new height decreased with the particle size.

Smaller particles will form larger bubble diameters. As the height above the air distributor increases, as can be seen from the experiment results, particles with  $D_p$  0.34mm still predominate the graph that form large bubbles and then followed by  $D_p$  2.71mm and  $D_p$  3.35mm. Large particles will have larger void friction in the packed bed column and thus affect the bubble diameter where the bubble diameter is expected to be smaller.

The results show that as pressure increases, the bubble diameter will increase gradually until a certain pressure where bubble diameter is maximum and after that bubble diameter will decrease even though pressure is increasing. Smaller particles will create large bubble diameters because smaller particles have smaller void friction that easily trap air and form big bubbles.

## **5.2 Recommendation**

The air flow at the plenum before enter fluidized bed is not center. Thus this result the bubble formation to form at the side of the fluidized bed and not in the middle fluidized bed. To cater this problem, the air tube that connected to the plenum was cut shorter and the length of air tube inside the plenum was made uniform.

Fluidized bed need to be repaired since the small light behind the fluidized bed cannot be used. Extra lighting was used to complete the experiment. Fluidized bed need to be install with temperature indicator to monitor inlet air temperature from the compressor.

Column can be vary by changing the column shape to circular, rectangular or triangle shape to examine the bubble characteristic inside those columns. More column shape provides more information for bubble characteristic inside the column.

The data for bubble diameter and bed expansion should be repeat at least three times to get more reliable and consistent values.

## REFERENCES

- Al-Zahrani, A. A., & Daous, M. A. (1996). Bed expansion and average bubble rise velocity in a gas-solid fluidized bed. *Powder Technology*, 87(3), 255-257. doi: 10.1016/0032-5910(96)03095-1
- Barletta, M., Bolelli, G., Gisario, A., & Lusvarghi, L. (2008). Mechanical strength and wear resistance of protective coatings applied by fluidized bed (FB). *Progress in Organic Coatings*, 61(2-4), 262-282. doi: 10.1016/j.porgcoat.2007.09.029
- Chew, J. W., Hays, R., Findlay, J. G., Knowlton, T. M., Reddy Karri, S. B., Cocco, R. A., & Hrenya, C. M. (2012). Cluster characteristics of geldart group B particles in a pilot-scale CFB riser. I. monodisperse systems. *Chemical Engineering Science*, 68(1), 72-81. doi: 10.1016/j.ces.2011.09.012
- Cody, G. D., Goldfarb, D. J., Storch Jr, G. V., & Norris, A. N. (1996). Particle granular temperature in gas fluidized beds. *Powder Technology*, 87(3), 211-232. doi: 10.1016/0032-5910(96)03087-2
- Cody, G. D., Johri, J., & Goldfarb, D. (2008). Dependence of particle fluctuation velocity on gas flow, and particle diameter in gas fluidized beds for monodispersed spheres in the geldart B and A fluidization regimes. *Powder Technology*, 182(2), 146-170. doi: 10.1016/j.powtec.2007.06.013
- da Cunha, R. L. G., Pereira, M. M. C., & Rocha, S. C. S. (2009). Conventional and modified fluidized bed: Comparison of the fluid dynamics and application in particle granulation. *Chemical Engineering and Processing: Process Intensification*, 48(5), 1004-1011. doi: 10.1016/j.cep.2009.01.005
- Gauthier, D., Zerguerras, S., & Flamant, G. (1999). Influence of the particle size distribution of powders on the velocities of minimum and complete fluidization. *Chemical Engineering Journal*, 74(3), 181-196. doi: 10.1016/S1385-8947(99)00075-3
- Gauthier, D., Zerguerras, S., & Flamant, G. (1999). Influence of the particle size distribution of powders on the velocities of minimum and complete fluidization. *Chemical Engineering Journal*, 74(3), 181-196. doi: 10.1016/S1385-8947(99)00075-3
- Girimonte, R., & Vivacqua, V. (2011). The expansion process of particle beds fluidized in the voids of a packing of coarse spheres. *Powder Technology*, 213(1-3), 63-69. doi: 10.1016/j.powtec.2011.07.006

- Gungor, A., & Eskin, N. (2007). Hydrodynamic modeling of a circulating fluidized bed. *Powder Technology*, 172(1), 1-13. doi: 10.1016/j.powtec.2006.10.035
- HILAL, N. (2005). The dependence of solid expansion on bed diameter, particles material, size and distributor in open fluidized beds. *Advanced Powder Technology*, 16(1), 73-86. doi: 10.1163/1568552053166692
- Jing, S., Hu, Q., Wang, J., & Jin, Y. (2000). Fluidization of coarse particles in gas–solid conical beds. *Chemical Engineering and Processing: Process Intensification*, 39(4), 379-387. doi: 10.1016/S0255-2701(99)00103-8
- Kozanoglu, B. U., Welti Chanes, J., García Cuautle, D., & Santos Jean, J. P. (2002). Hydrodynamics of large particle fluidization in reduced pressure operations: An experimental study. *Powder Technology*, 125(1), 55-60. doi: 10.1016/S0032-5910(01)00524-1
- Li, H., Lu, X., & Kwauk, M. (2003). Particulation of gas–solids fluidization. *Powder Technology*, 137(1–2), 54-62. doi: 10.1016/j.powtec.2003.08.030
- Lim, K. S., Zhu, J. X., & Grace, J. R. (1995). Hydrodynamics of gas-solid fluidization. *International Journal of Multiphase Flow*, 21, Supplement(0), 141-193. doi: 10.1016/0301-9322(95)00038-Y
- Liu, Y., Wang, T., Qin, L., & Jin, Y. (2008). Urea particle coating for controlled release by using DCPD modified sulfur. *Powder Technology*, 183(1), 88-93. doi: 10.1016/j.powtec.2007.11.022
- Llop, M. F., Casal, J., & Arnaldos, J. (2000). Expansion of gas–solid fluidized beds at pressure and high temperature. *Powder Technology*, 107(3), 212-225. doi: 10.1016/S0032-5910(99)00188-6
- Lu, S. M., Chang, S., Ku, W., Chang, H., Wang, J., & Lee, D. (2007). Urea release rate from a scoop of coated pure urea beads: Unified extreme analysis. *Journal of the Chinese Institute of Chemical Engineers*, 38(3–4), 295-302. doi: 10.1016/j.jcice.2007.04.001
- Ng, W. K., & Tan, R. B. H. (2008). Case study: Optimization of an industrial fluidized bed drying process for large geldart type D nylon particles. *Powder Technology*, 180(3), 289-295. doi: 10.1016/j.powtec.2007.02.020
- Parise, M. R., Silva, C. A. M., Ramazini, M. J., & Taranto, O. P. (2011). Identification of defluidization in fluidized bed coating using the gaussian spectral pressure distribution. *Powder Technology*, 206(1–2), 149-153. doi: 10.1016/j.powtec.2010.07.008

- Qi, X., Zhu, J., & Huang, W. (2008). Hydrodynamic similarity in circulating fluidized bed risers. *Chemical Engineering Science*, 63(23), 5613-5625. doi: 10.1016/j.ces.2008.07.036
- Rong, L., Zhan, J., & Wu, C. (2012). Effect of various parameters on bubble formation due to a single jet pulse in two-dimensional coarse-particle fluidized beds. *Advanced Powder Technology*, 23(3), 398-405. doi: 10.1016/j.apt.2011.05.008
- Roy, P., Khanna, R., & Subbarao, D. (2010). Granulation time in fluidized bed granulators. *Powder Technology*, 199(1), 95-99. doi: 10.1016/j.powtec.2009.04.018
- Sakai, M., Takahashi, H., Pain, C. C., Latham, J., & Xiang, J. Study on a large-scale discrete element model for fine particles in a fluidized bed. *Advanced Powder Technology*, (0) doi: 10.1016/j.apt.2011.08.006
- Shuai, W., Zhenhua, H., Huilin, L., Yunchao, Y., Pengfei, X., & Guodong, L. (2012). Hydrodynamic modeling of particle rotation in bubbling gas-fluidized beds. *International Journal of Multiphase Flow*, 39(0), 159-178. doi: 10.1016/j.ijmultiphaseflow.2011.09.007
- Sidorenko, I., & Rhodes, M. J. (2004). Influence of pressure on fluidization properties. *Powder Technology*, 141(1-2), 137-154. doi: 10.1016/j.powtec.2004.02.019
- Silva, C. A. M., Parise, M. R., Silva, F. V., & Taranto, O. P. (2011). Control of fluidized bed coating particles using gaussian spectral pressure distribution. *Powder Technology*, 212(3), 445-458. doi: 10.1016/j.powtec.2011.07.007
- Singh, R. K., & Roy, G. K. (2005). Prediction of minimum bubbling velocity, fluidization index and range of particulate fluidization for gas-solid fluidization in cylindrical and non-cylindrical beds. *Powder Technology*, 159(3), 168-172. doi: 10.1016/j.powtec.2005.08.008
- Sobrino, C., Acosta-Iborra, A., Santana, D., & de Vega, M. (2009). Bubble characteristics in a bubbling fluidized bed with a rotating distributor. *International Journal of Multiphase Flow*, 35(10), 970-976. doi: 10.1016/j.ijmultiphaseflow.2009.04.005
- Sobrino, C., Almendros-Ibañez, J. A., Santana, D., & de Vega, M. (2008). Fluidization of group B particles with a rotating distributor. *Powder Technology*, 181(3), 273-280. doi: 10.1016/j.powtec.2007.05.014
- Subramani, H. J., Mothivel Balaiyya, M. B., & Miranda, L. R. (2007). Minimum fluidization velocity at elevated temperatures for Geldart's group-B powders. *Experimental Thermal and Fluid Science*, 32(1), 166-173. doi: 10.1016/j.expthermflusci.2007.03.003

- Subramani, H. J., Mothivel Balaiyya, M. B., & Miranda, L. R. (2007). Minimum fluidization velocity at elevated temperatures for Geldart's group-B powders. *Experimental Thermal and Fluid Science*, 32(1), 166-173. doi: 10.1016/j.expthermflusci.2007.03.003
- Tzika, M., Alexandridou, S., & Kiparissides, C. (2003). Evaluation of the morphological and release characteristics of coated fertilizer granules produced in a wurster fluidized bed. *Powder Technology*, 132(1), 16-24. doi: 10.1016/S0032-5910(02)00345-5
- Van den Moortel, T., Azario, E., Santini, R., & Tadriss, L. (1998). Experimental analysis of the gas-particle flow in a circulating fluidized bed using a phase doppler particle analyzer. *Chemical Engineering Science*, 53(10), 1883-1899. doi: 10.1016/S0009-2509(98)00030-X
- W.J., L. (1996). Liquid fluidized bed coating process. *Carbon*, 34(10), 1299-1300. doi: 10.1016/0008-6223(96)82801-6
- Wiman, J., & Almstedt, A. E. (1998). Influence of pressure, fluidization velocity and particle size on the hydrodynamics of a freely bubbling fluidized bed. *Chemical Engineering Science*, 53(12), 2167-2176. doi: 10.1016/S0009-2509(98)00056-6
- Xu, C., & Zhu, J. -. (2006). Effects of gas type and temperature on fine particle fluidization. *China Particuology*, 4(3-4), 114-121. doi: 10.1016/S1672-2515(07)60249-8
- Xu, C., & Zhu, J. -. (2006). Effects of gas type and temperature on fine particle fluidization. *China Particuology*, 4(3-4), 114-121. doi: 10.1016/S1672-2515(07)60249-8
- Xu, G., Nomura, K., Nakagawa, N., & Kato, K. (2000). Hydrodynamic dependence on riser diameter for different particles in circulating fluidized beds. *Powder Technology*, 113(1-2), 80-87. doi: 10.1016/S0032-5910(99)00317-4
- Yang, W. (2007). Modification and re-interpretation of geldart's classification of powders. *Powder Technology*, 171(2), 69-74. doi: 10.1016/j.powtec.2006.08.024

## APPENDIX

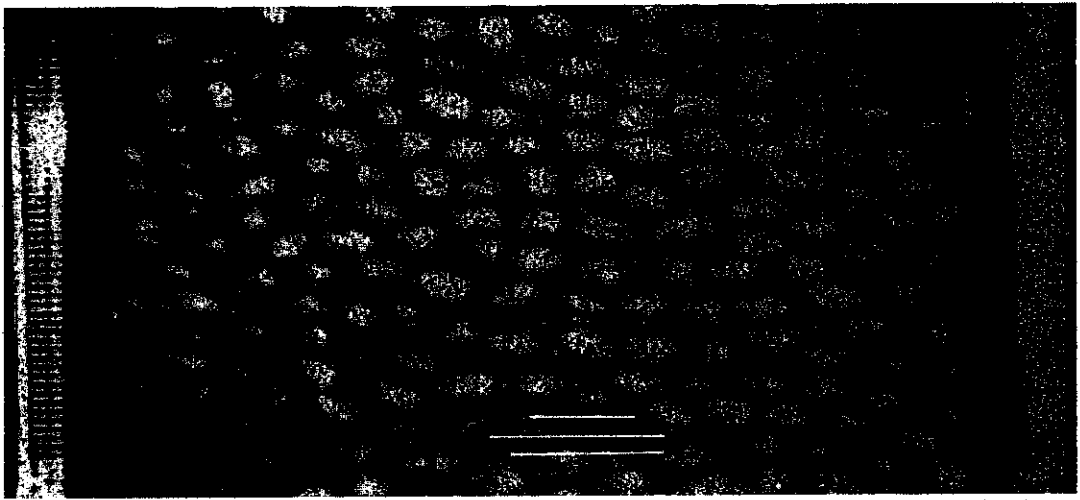


Figure 1: Bubble diameter distribution for height above air distributor,  $D_p = 2.71$  mm, Pressure = 0.3 bar,  $H_{mf} = 10$  cm

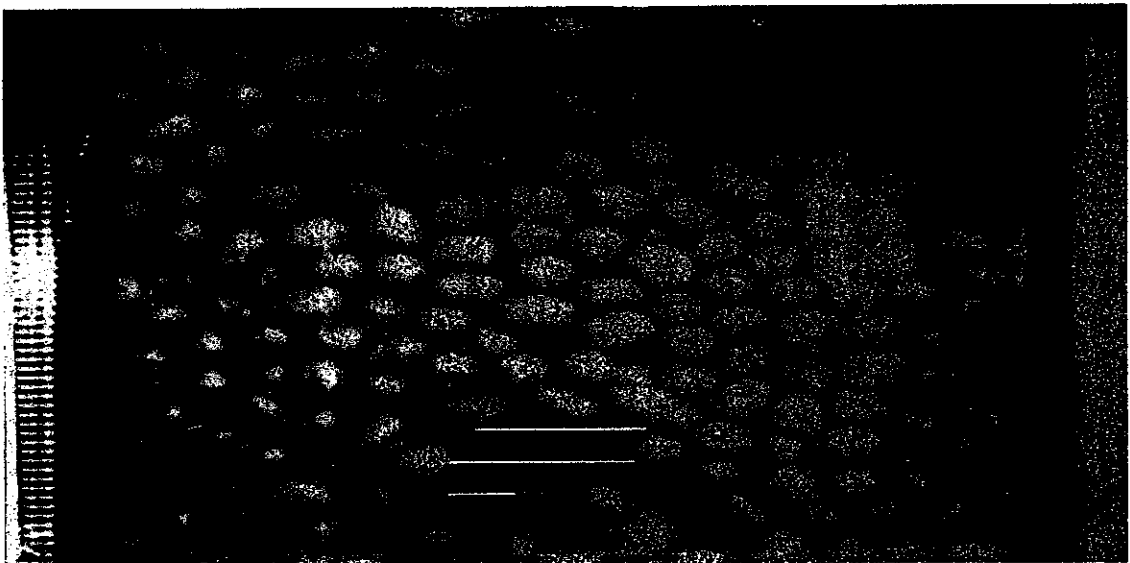


Figure 2 : Bubble diameter distribution for height above air distributor,  $D_p = 2.71$  mm Pressure = 0.3 bar  $H_{mf} = 20$  cm

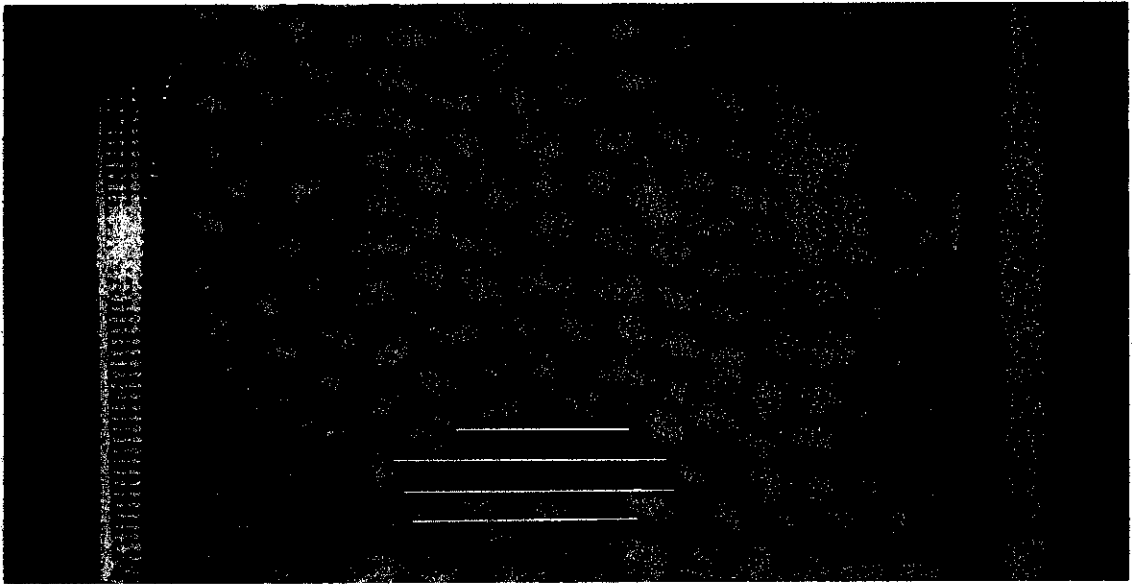


Figure 3 : Bubble diameter distribution for height above air distributor,  $D_p = 2.71$  mm  
Pressure = 0.3 bar  $H_{mf} = 30$ cm

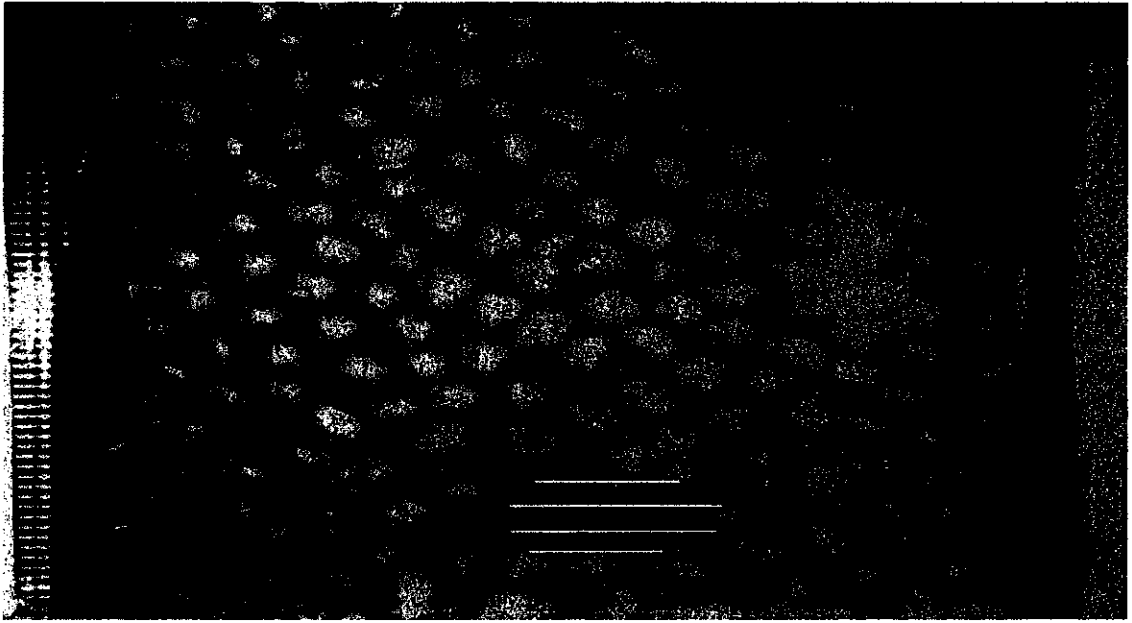


Figure 4 : Bubble diameter distribution for height above air distributor,  $D_p = 2.71\text{mm}$   
Pressure = 0.5 bar,  $H_{mf} = 10\text{cm}$

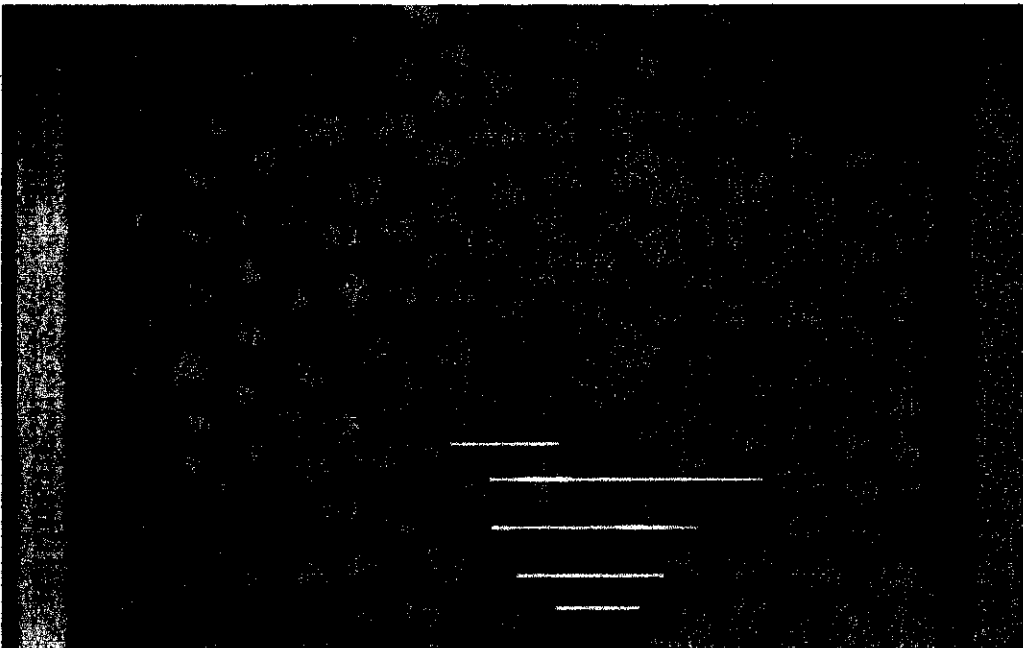


Figure 5 : Bubble diameter distribution for height above air distributor,  $D_p = 2.71\text{mm}$   
Pressure = 0.5 bar,  $H_{mf} = 20\text{cm}$

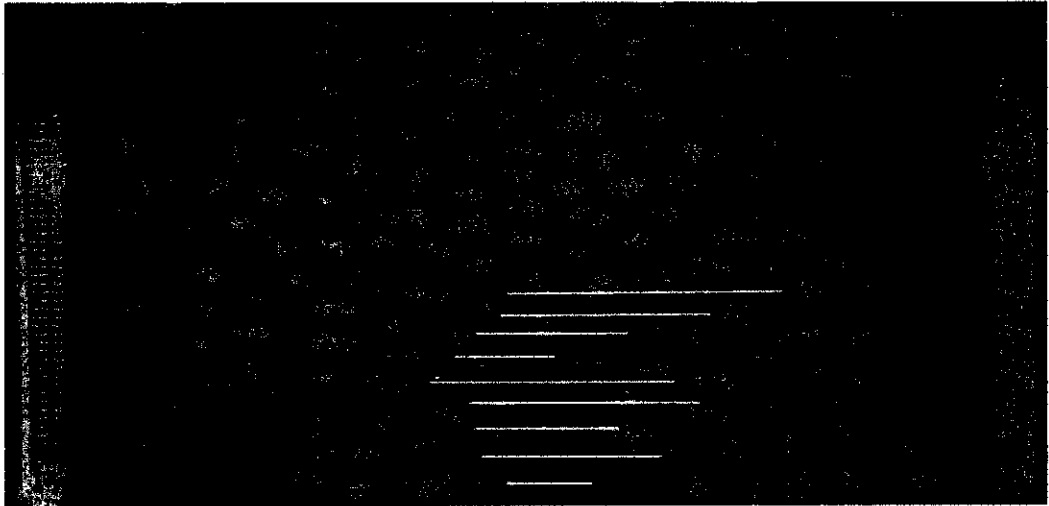


Figure 6 : Bubble diameter distribution for height above air distributor  $D_p = 2.71\text{mm}$   
Pressure = 0.5 bar,  $H_{mf} = 30\text{cm}$

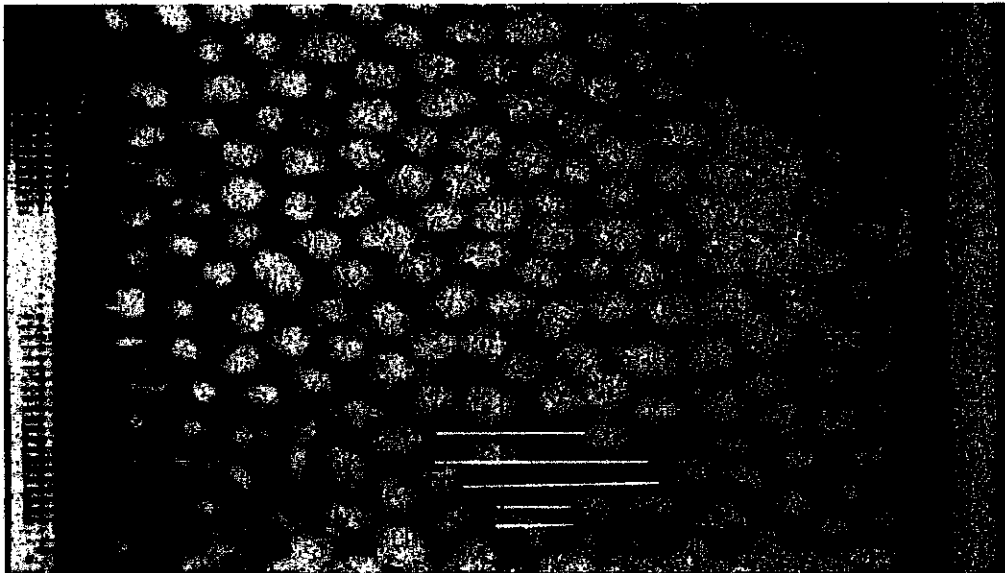


Figure 7 : Bubble diameter distribution for height above air distributor  $D_p = 2.71\text{mm}$   
Pressure = 0.7 bar,  $H_{mf} = 10\text{cm}$

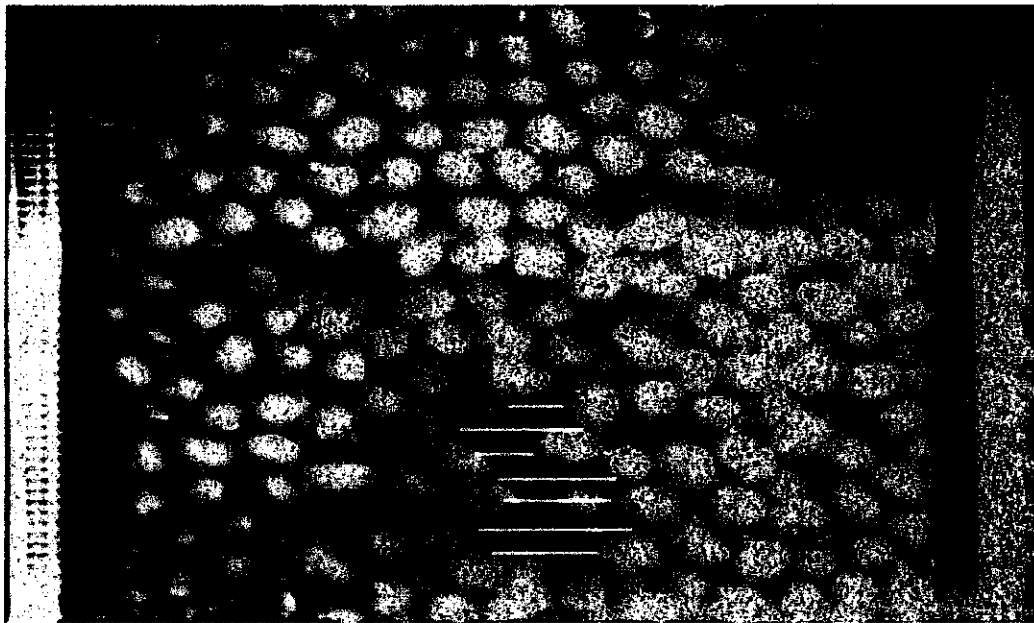


Figure 8 : Bubble diameter distribution for height above air distributor  $D_p = 2.71\text{mm}$   
Pressure = 0.7 bar,  $H_{mf} = 20\text{cm}$



Figure 9 : Bubble diameter distribution for height above air distributor  $D_p = 2.71\text{mm}$   
Pressure = 0.7 bar,  $H_{mf} = 30\text{cm}$

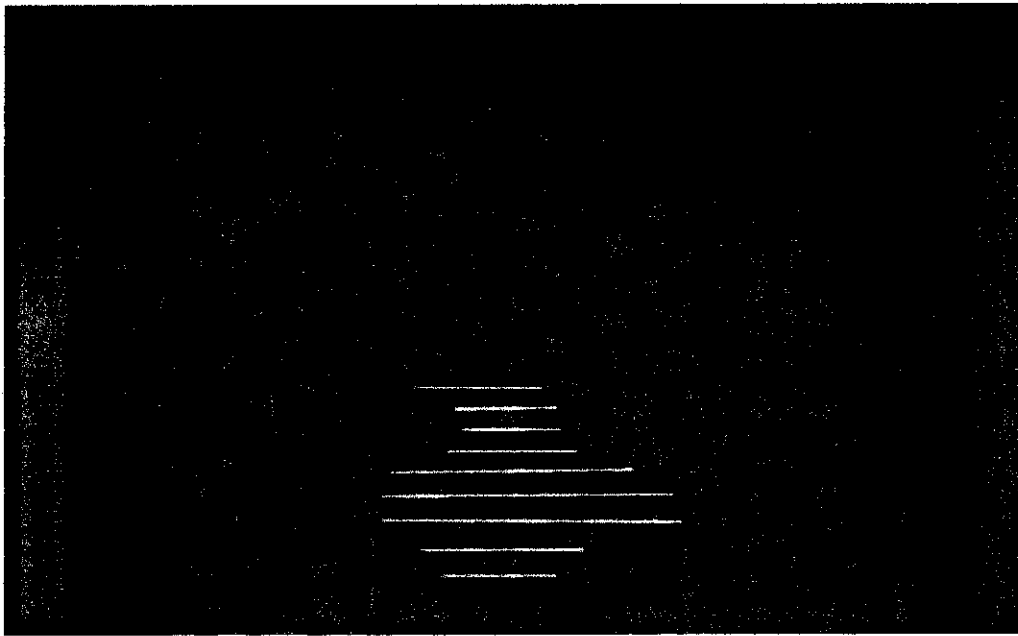


Figure 10 : Bubble diameter distribution for height above air distributor  $D_p = 2.71\text{mm}$   
Pressure = 0.9 bar,  $H_{mf} = 10\text{cm}$

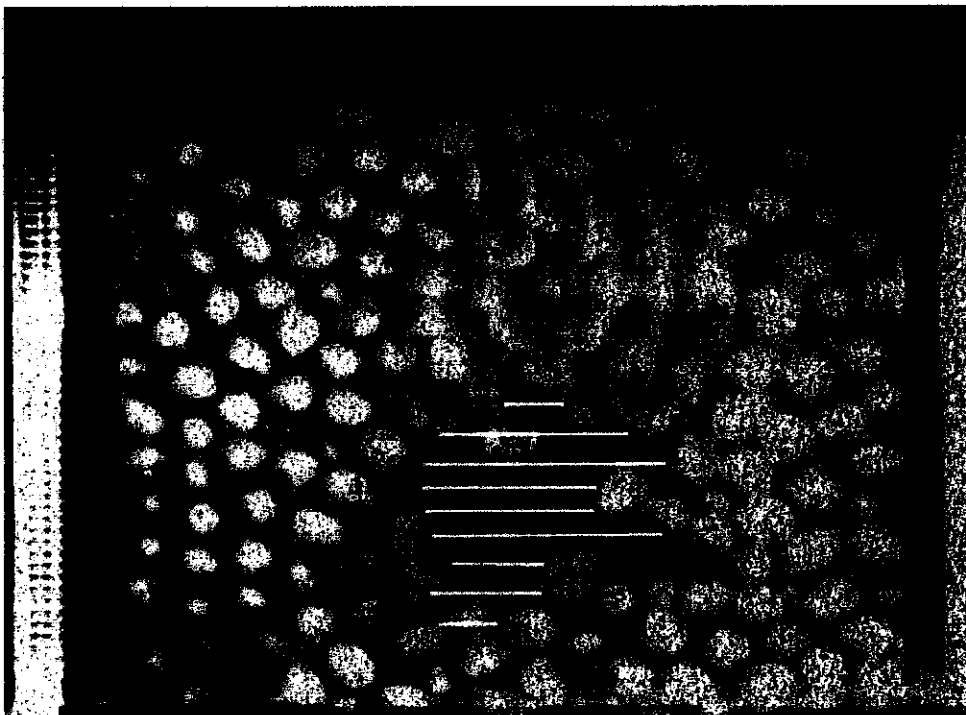


Figure 11 : Bubble diameter distribution for height above air distributor  $D_p = 2.71\text{mm}$   
Pressure = 0.9 bar,  $H_{mf} = 20\text{cm}$

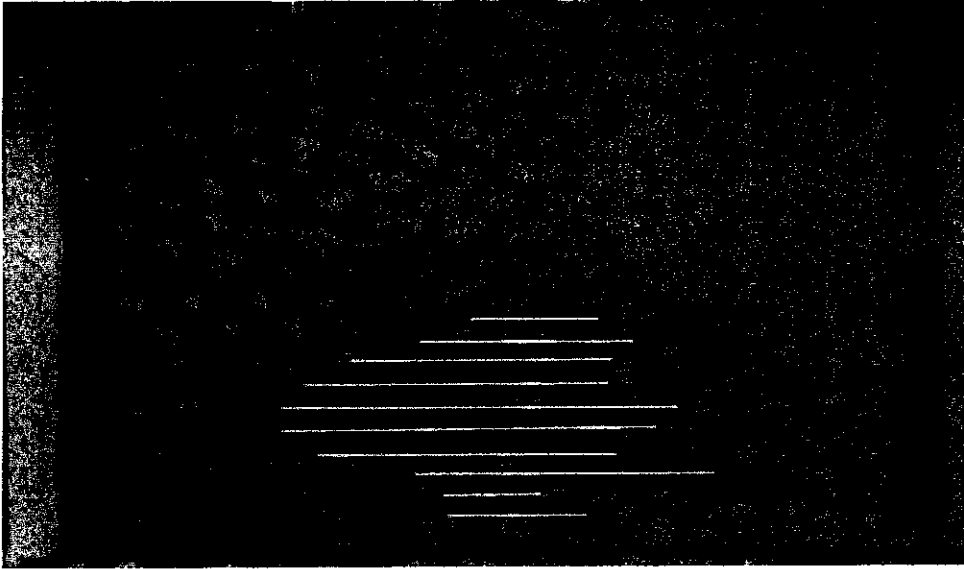


Figure 12 : Bubble diameter distribution for height above air distributor  $D_p = 2.71\text{mm}$   
Pressure = 0.9 bar,  $H_{mf} = 30\text{cm}$

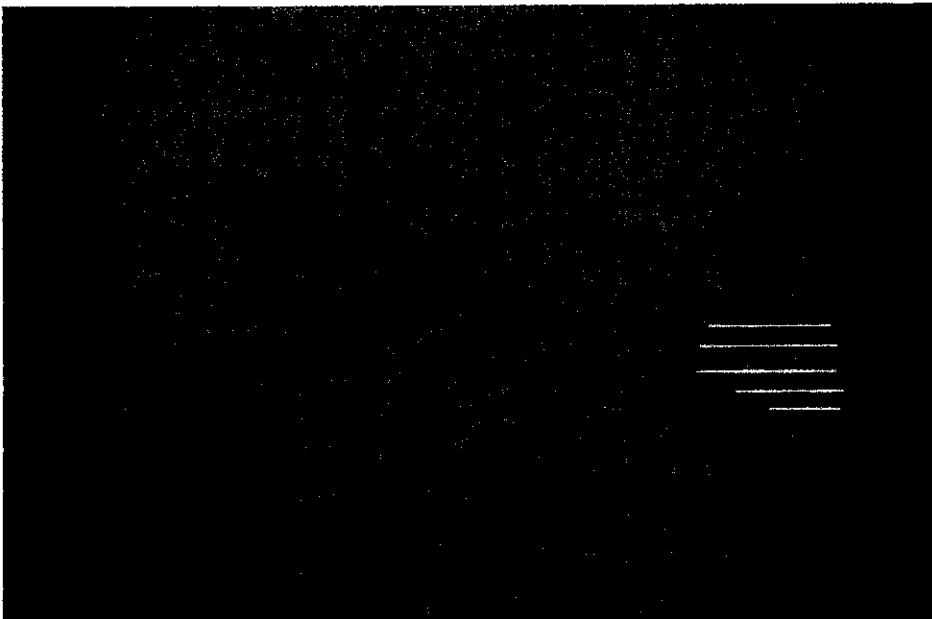


Figure 13 : Bubble diameter distribution for height above air distributor  $D_p = 3.35\text{mm}$   
Pressure = 0.3 bar,  $H_{mf} = 10\text{cm}$

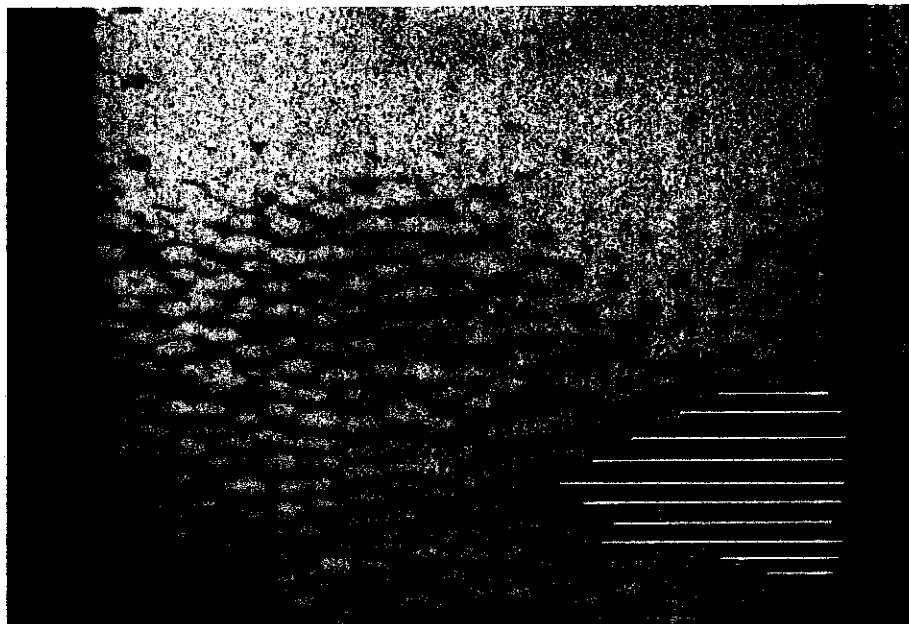


Figure 14 : Bubble diameter distribution for height above air distributor  $D_p = 3.35\text{mm}$   
Pressure = 0.3 bar,  $H_{mf} = 20\text{cm}$

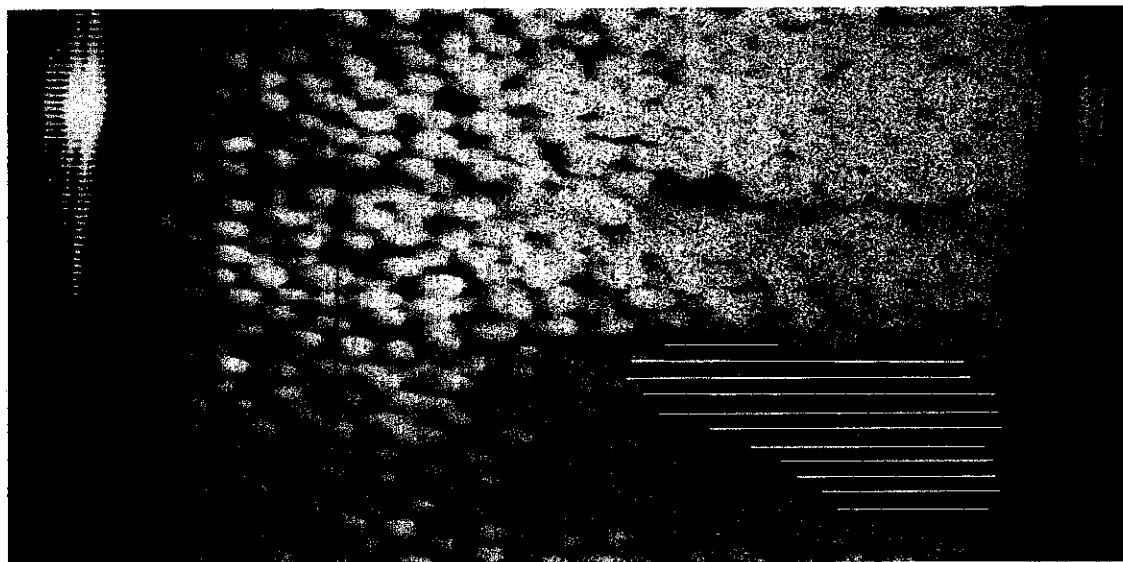


Figure 15 : Bubble diameter distribution for height above air distributor  $D_p = 3.35\text{mm}$   
Pressure = 0.3 bar,  $H_{mf} = 30\text{cm}$

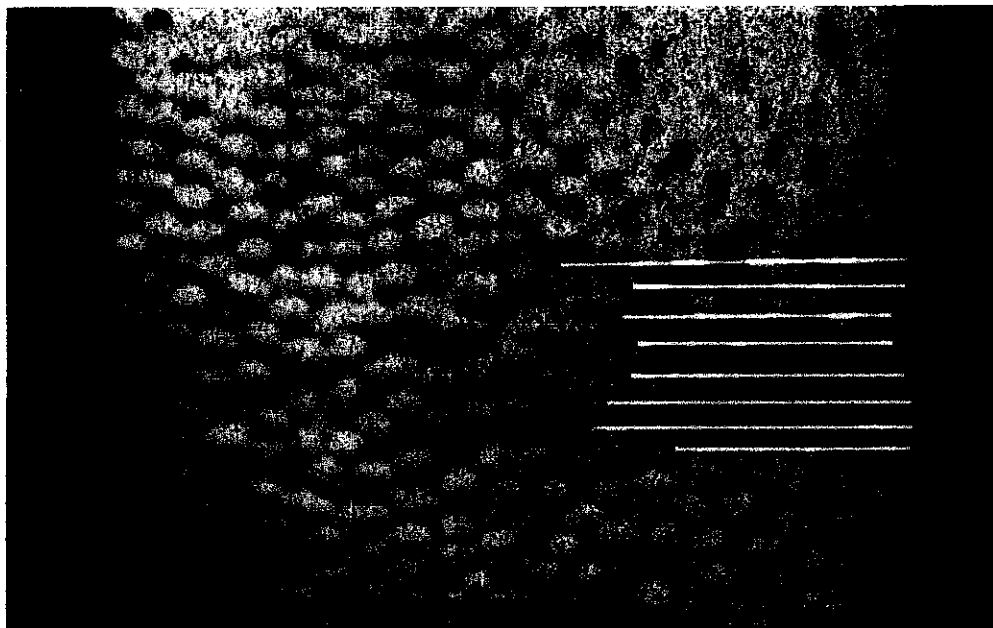


Figure 16 : Bubble diameter distribution for height above air distributor  $D_p = 3.35\text{mm}$   
Pressure = 0.5 bar,  $H_{mf} = 10\text{cm}$

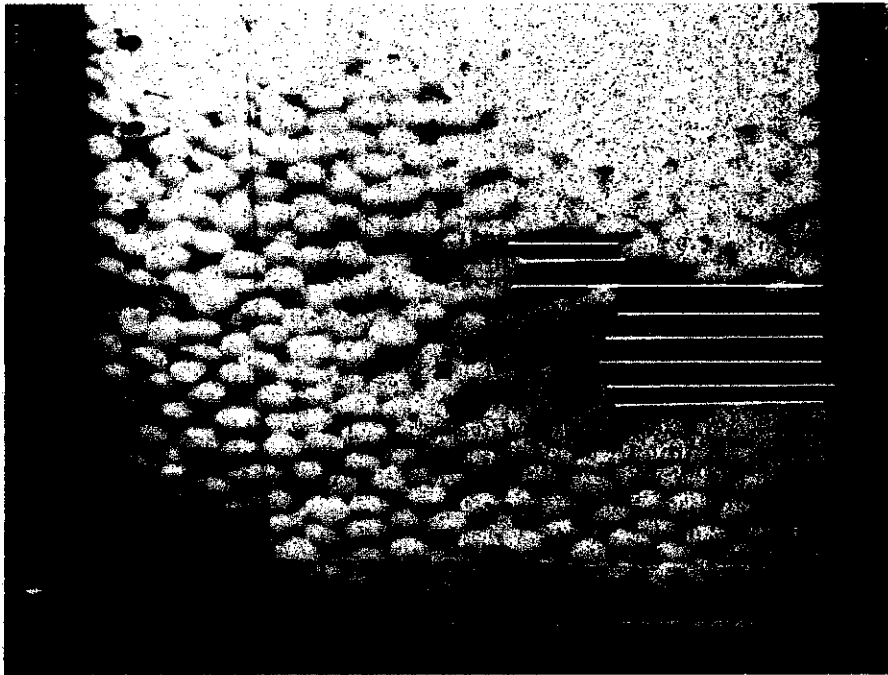


Figure 17 : Bubble diameter distribution for height above air distributor  $D_p = 3.35\text{mm}$   
Pressure = 0.5 bar,  $H_{mf} = 20\text{cm}$

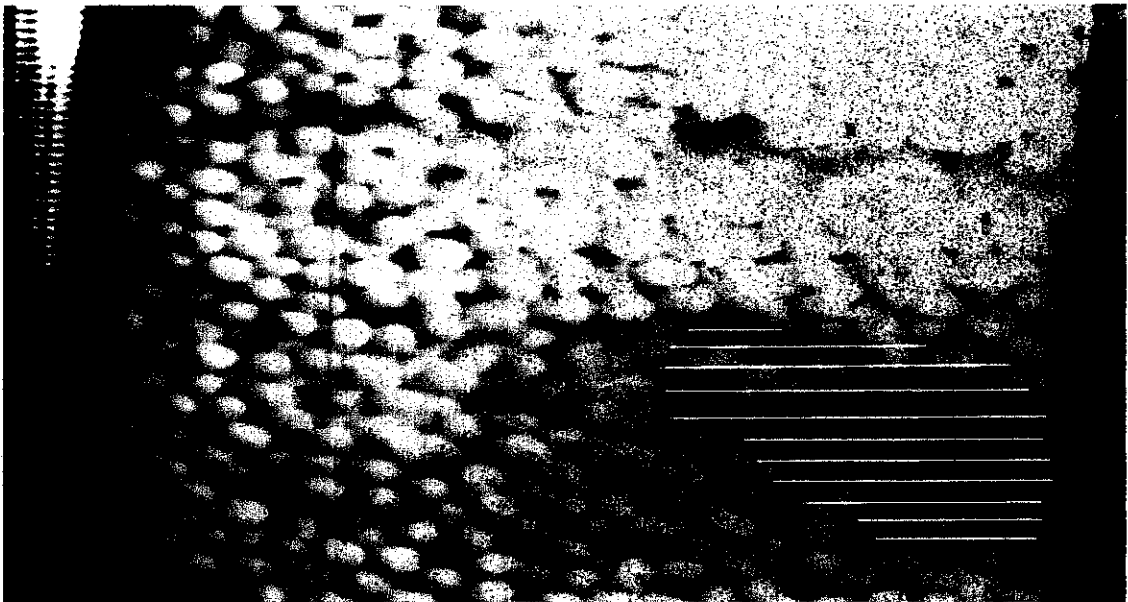


Figure 18 : Bubble diameter distribution for height above air distributor  $D_p = 3.35\text{mm}$   
Pressure = 0.5 bar,  $H_{mf} = 30\text{cm}$

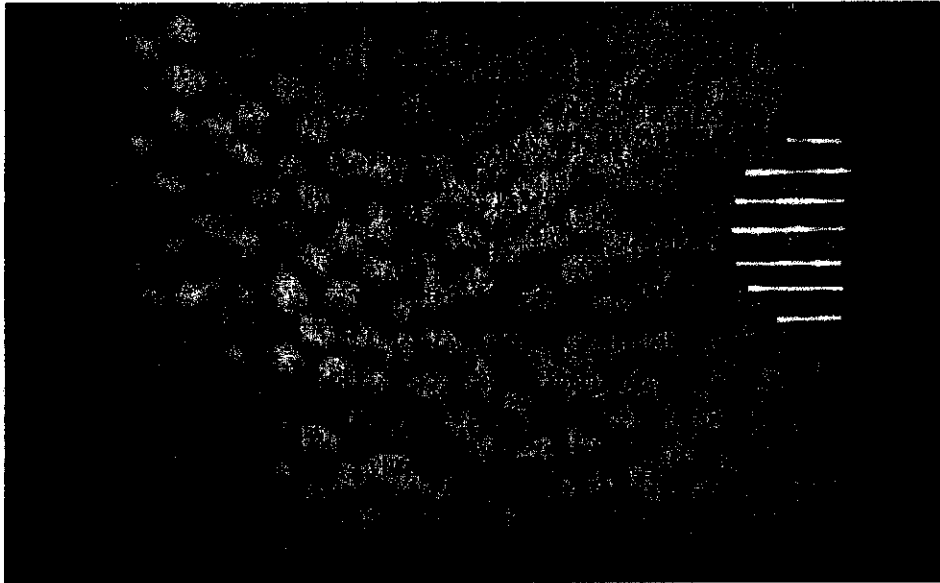


Figure 19 : Bubble diameter distribution for height above air distributor  $D_p = 3.35\text{mm}$   
Pressure = 0.7 bar,  $H_{mf} = 10\text{cm}$

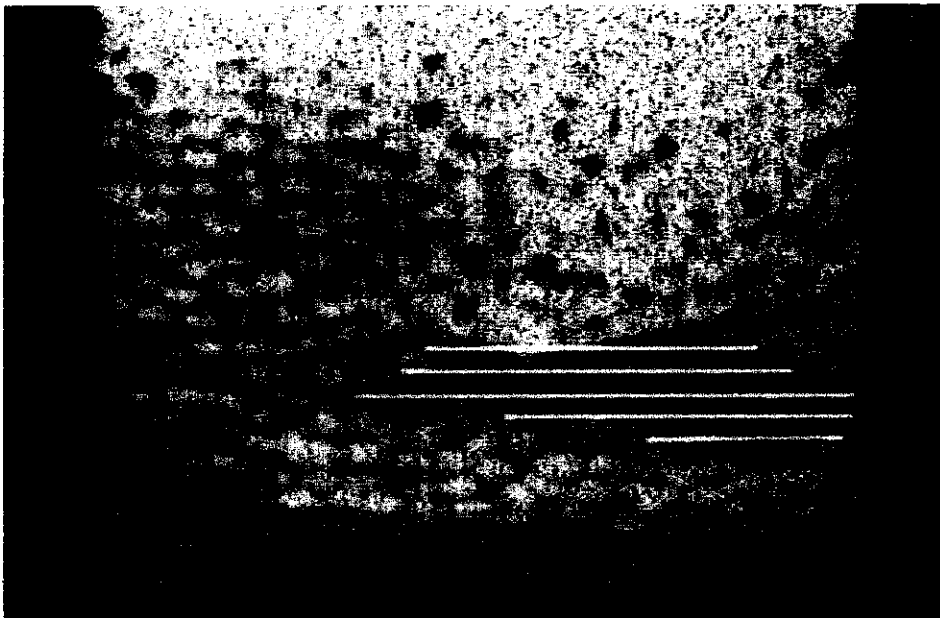


Figure 20 : Bubble diameter distribution for height above air distributor  $D_p = 3.35\text{mm}$   
Pressure = 0.7 bar,  $H_{mf} = 20\text{cm}$



Figure 21 : Bubble diameter distribution for height above air distributor  $D_p = 3.35\text{mm}$   
 Pressure = 0.7 bar,  $H_{mf} = 30\text{cm}$



Figure 22: Bubble diameter distribution for height above air distributor  $D_p = 3.35\text{mm}$   
 Pressure = 0.9 bar,  $H_{mf} = 10\text{cm}$

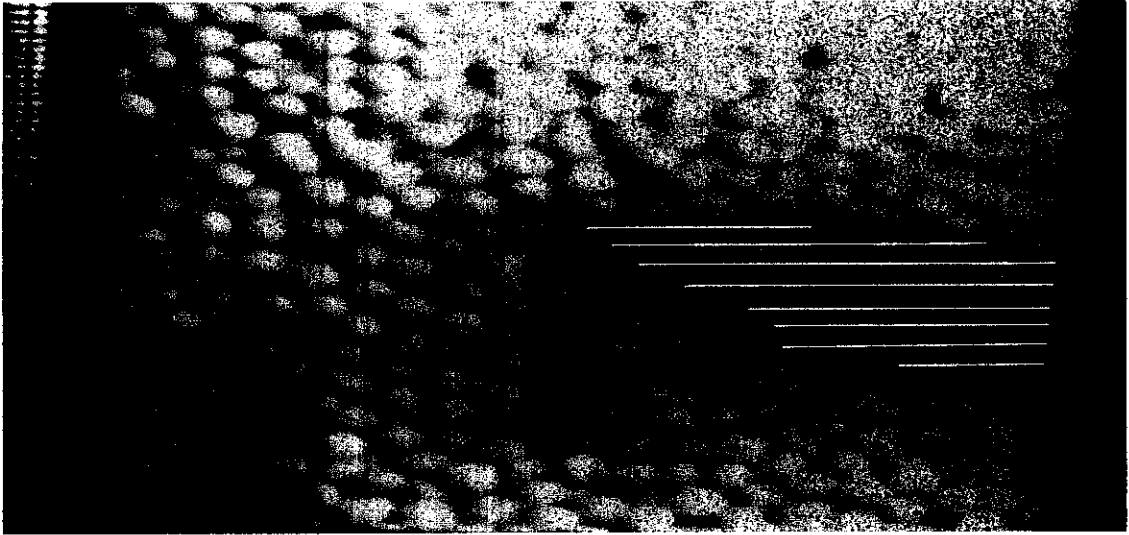


Figure 23 : Bubble diameter distribution for height above air distributor  $D_p = 3.35\text{mm}$   
Pressure = 0.9 bar,  $H_{mf} = 20\text{cm}$

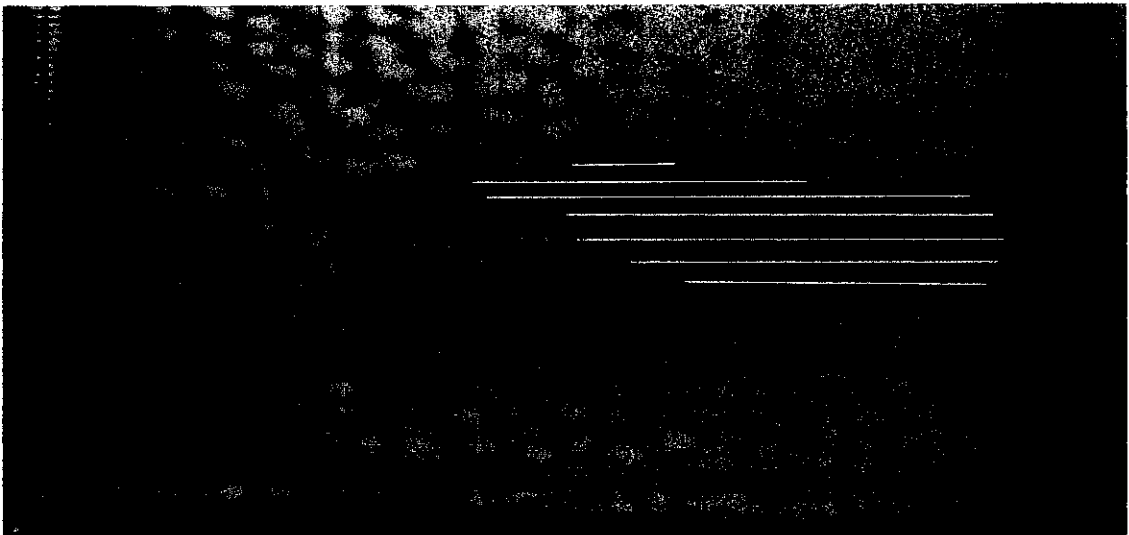


Figure 24 : Bubble diameter distribution for height above air distributor  $D_p = 3.35\text{mm}$   
Pressure = 0.9 bar,  $H_{mf} = 30\text{cm}$



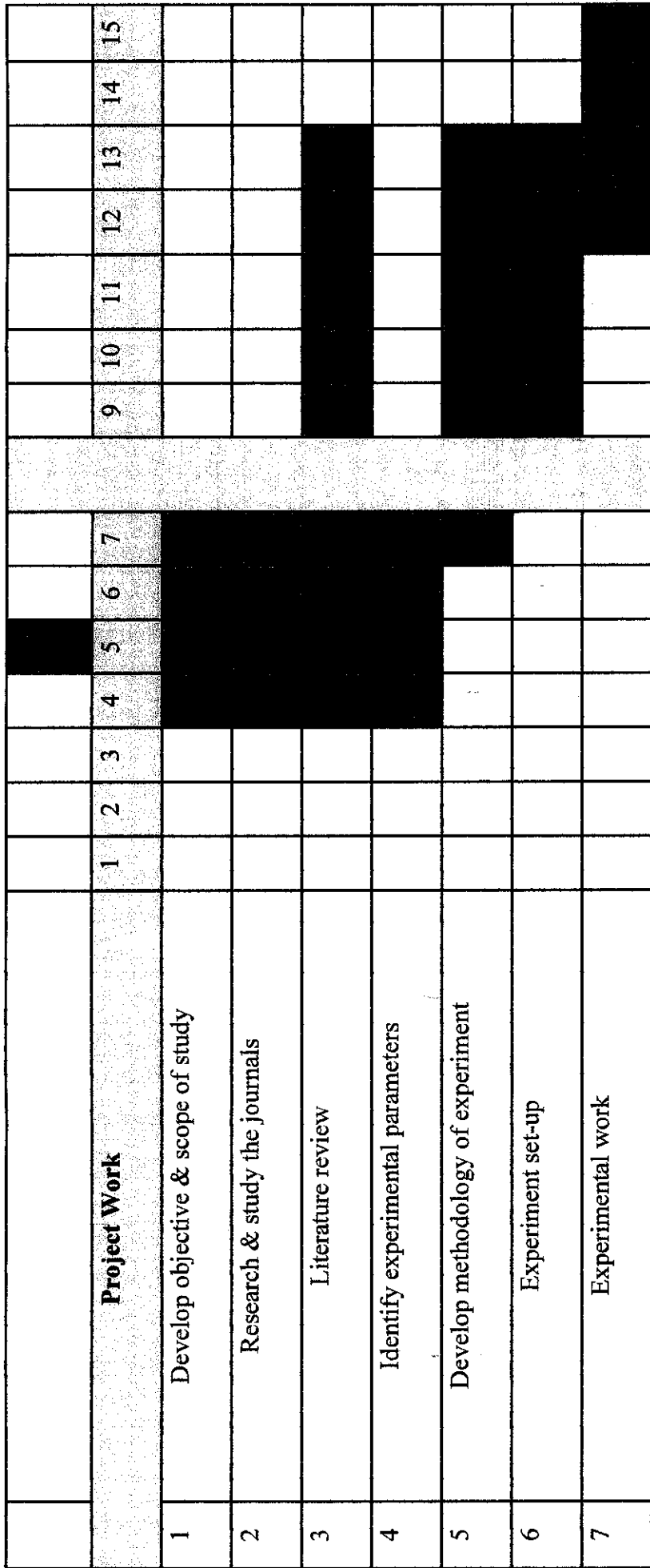


Figure 25: Project Gant Chart